City of Morro Bay and
Cayucos Sanitary District

OFFSHORE MONITORING AND REPORTING PROGRAM

QUARTERLY REPORT

WATER-COLUMN SAMPLING JULY 2007 SURVEY

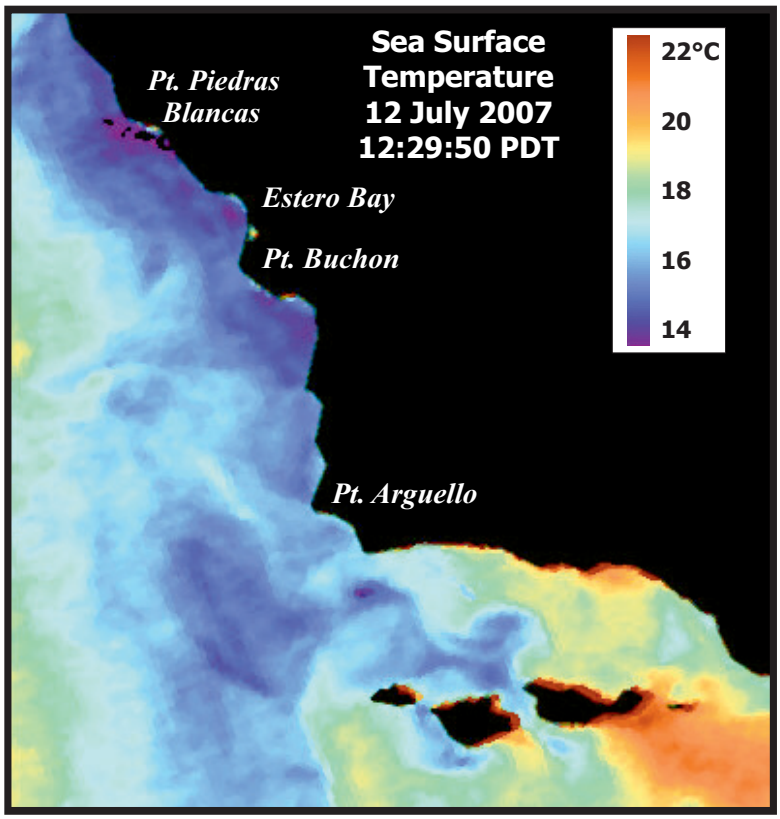

Marine Research Specialists

3140 Telegraph Rd., Suite A
Ventura, California 93003

Report to

City of Morro Bay and
Cayucos Sanitary District

955 Shasta Avenue
Morro Bay, California 93442
(805) 772-6272

OFFSHORE MONITORING AND REPORTING PROGRAM

QUARTERLY REPORT

WATER-COLUMN SAMPLING JULY 2007

Prepared by

Douglas A. Coats
Tyler Eck
Bonnie Luke

Marine Research Specialists

3140 Telegraph Rd., Suite A
Ventura, California 93003

Telephone: (805) 644-1180
Telefax: (805) 289-3935
E-mail: Doug.Coats@mrsenv.com

August 2007

marine research specialists
3140 Telegraph Road, Suite A · Ventura, CA 93003 · (805) 644-1180

Mr. Bruce Keogh
Wastewater Division Manager
City of Morro Bay
955 Shasta Avenue
Morro Bay, CA 93442

29 August 2007

Reference: Quarterly Receiving-Water Report – July 2007

Dear Mr. Keogh:

Enclosed is the Quarterly Report for the Water-Quality Survey conducted on Friday, 6 July 2007. This third-quarter survey assessed the effectiveness of effluent dispersion during summer oceanographic conditions. Based on quantitative analyses of continuous instrumental measurements and qualitative visual observations, the wastewater discharge was found to be in compliance with the receiving-water limitations specified in the NPDES discharge permit, and with the objectives of the California Ocean Plan.

High-precision measurements clearly delineated discharge-related perturbations in all six seawater properties at one of the sixteen sampling stations. The station was located along the boundary of the zone of initial dilution to the north of the diffuser structure, and in a direction consistent with plume transport by prevailing currents. The anomalies in three of the seawater properties were generated by the upward displacement of ambient seawater entrained within the rising effluent plume. Variations in the other three seawater properties reflected the presence of very dilute wastewater constituents that were continuing to undergo vigorous mixing. Dilution levels determined from the salinity anomaly within the discharge plume significantly exceeded those anticipated by modeling and outfall design criteria. Thus, all of the measurements were indicative of low organic loading within the discharged wastewater, and of an outfall operating as designed.

Please contact the undersigned if you have any questions regarding the attached report.

Sincerely,

Douglas A. Coats, Ph.D.
Program Manager

Enclosure (Five Report Copies)

I certify under penalty of law that this document and all attachments were prepared under my direction or supervision in accordance with a system designed to assure that qualified personnel properly gather and evaluate the information submitted. Based on my inquiry of the person or persons who manage the system, or those persons directly responsible for gathering the information, the information submitted is, to the best of my knowledge and belief, true, accurate, and complete. I am aware that there are significant penalties for submitting false information, including the possibility of fine and imprisonment for knowing violations.

_____

Mr. Bruce Ambo
City of Morro Bay

Date _____

TABLE OF CONTENTS

LIST OF FIGURES

LIST OF TABLES

INTRODUCTION

The City of Morro Bay and the Cayucos Sanitary District (MBCSD) jointly own the wastewater treatment plant operated by the City of Morro Bay. A National Pollutant Discharge Elimination System (NPDES) permit, modifying secondary treatment requirements, was originally issued to the MBCSD in March 1985. The permit was issued by Region IX of the U.S. Environmental Protection Agency (USEPA) and the Central Coast California Regional Water Quality Control Board (RWQCB). Following extensive evaluation processes, the permit has been re-issued twice, once in March of 1993 (RWQCB-USEPA 1993ab) and again in December 1998 (RWQCB-USEPA 1998ab).

As part of the current permit provisions, the previous monitoring program was modified to better evaluate short and long-term effects of the discharge on receiving waters, benthic sediments, and infaunal communities (RWQCB-EPA 1998b). The program continued to include a requirement for receiving-water-quality monitoring performed on a seasonal basis. The four quarterly surveys are intended to record ambient water properties that approximate winter, spring, summer, and fall conditions. In keeping with seasonal synopses, this quarterly report summarizes the results of water-quality sampling conducted on 6 July 2007. Specifically, this third-quarter survey captures ambient oceanographic conditions along the central California coast during the summer season.

The water-quality surveys also provide timely assessments of the performance of the diffuser structure in dispersing wastewater within stratified receiving waters. Any significant, recent damage to the diffuser structure would be revealed by a decline in the level of wastewater dispersion measured in this survey compared to that of prior surveys, and compared to design specifications. As described in this report, no such decline was observed in the July 2007 field survey.

Both monitoring objectives were achieved through an evaluation of the water-column profiles and cross sections of water-property distributions that are presented in Appendix A. Appendix B tabulates instrumental measurements and standard field observations. These data were used to assess compliance with the objectives of the California Ocean Plan (COP) as promulgated by the NPDES discharge permit.

The July 2007 field survey was the thirty-fifth receiving-water survey to be conducted under the monitoring provisions of the current permit. Compared to the previous permit, the number of stations increased from 11 to 16, and the stations were relocated closer (≤100 m) to the diffuser structure. Sampling at these more closely spaced stations could only be achieved because of the availability of increased navigational accuracy that resulted from implementation of the differential global positioning satellite (DGPS) system. This system was commissioned during the March 1998 survey (MRS 1998a) and was subsequently employed in the precise determination of the open section of the diffuser structure during a diver survey on 29 September 1998 (MRS 1998bc).

The current sampling design also allowed surveying to be conducted more rapidly than previous surveys by eliminating the requirement for collection of discrete water samples at individual stations. These samples were collected using Niskin bottles, which was time consuming and interrupted the continuity of instrumental measurements collected by the CTD[1] instrument package. Continuous deployment of the CTD between stations now provides a more synoptic snapshot of the water properties immediately

[1] Conductivity, Temperature, and Depth (CTD) were the original measurements recorded by this standard oceanographic instrument package, but the moniker now connotes an electronic instrument package with a broader suite of probes and sensors capable of *in situ* measurement of dissolved oxygen, transmissivity, and pH.

surrounding the diffuser structure. Consequently, the extent of the effluent plume and the amplitude of its associated water-property anomalies can be more precisely determined. The sensitive sensors onboard the CTD instrument package are capable of detecting minute changes in water properties. These sensors are described in the Methods Section below.

Surveys conducted prior to 1999 rarely detected the effluent plume because sampling stations were too widely separated to resolve a dilute wastewater signature that is highly localized around the outfall diffuser. With the implementation of the current sampling design in 1999, the presence of well-mixed effluent near the diffuser structure was found in all 35 of the subsequent water-quality surveys (MRS 2000, 2001, 2002, 2003, 2004, 2005, 2006, 2007), including the one described in this report. Moreover, improved navigation in concert with the denser sampling pattern more precisely delineated the lateral extent of the discharge-related perturbations in seawater properties.

Precision navigation is important for assessing compliance because most receiving-water limitations apply only beyond the narrow zone of initial dilution (ZID) that surrounds the outfall. Additionally, the amplitudes of the effluent-related perturbations can be better determined by the denser sampling pattern. The amplitudes of discharge-related salinity anomalies reveal the details of dilution as the effluent plume disperses within receiving waters. Measured dilution factors lend insight into the current operational performance of the outfall and diffuser structure. As described in this report, the presence of dilute effluent undergoing turbulent mixing within a strongly stratified water column north of the diffuser structure was delineated by the data collected during the July 2007 survey.

STATION LOCATIONS

The water-sampling stations surround the area where effluent is discharged within Estero Bay (Figure 1). The 1,450 m long outfall pipe, which carries the effluent from the onshore treatment plant, terminates at the diffuser structure, which lies on the seafloor approximately 827 m from the shoreline.[2] The diffuser structure itself extends an additional 52 m toward the northwest from the outfall terminus.

Twenty-eight of the 34 available ports discharge effluent along a 42 m section of the diffuser structure. The other six diffuser ports remain closed to improve dispersion by increasing the ejection velocity from the open ports. For a given flow rate, the diffuser ports were hydraulically designed to create a turbulent ejection jet, which serves to rapidly mix effluent with receiving seawater immediately upon discharge. Additional turbulent mixing occurs as the buoyant plume of dilute effluent rises through the water column. Most of this buoyancy-induced mixing occurs within a zone of initial dilution (ZID), whose lateral extent in modeling studies is considered to be approximately 15 m from the centerline of the diffuser structure. Beyond the ZID, the energetic waves, tides, and coastal currents within Estero Bay further disperse the discharge plume within the open-ocean receiving waters. Areas of special concern, such as sanctuaries and estuaries, are too distant to be affected by the effluent discharge. For example, the southern boundary of the Monterey Bay National Marine Sanctuary is located 38 km to the north, near Cambria Rock.

[2] This distance was determined from a navigational survey conducted on 6 July 2005 to benchmark the locations of the current surfzone sampling stations along the shoreline adjacent to the diffuser structure. The beginning of the section of the diffuser structure containing open diffuser ports lies directly offshore surfzone Station C (Figure 1). This closest-approach shoreline position was determined at the water's edge when the tidal level was +2.7 ft, referenced to mean lower low water (MLLW).

Figure 1. Regional Setting of Receiving-Water Sampling Stations within Estero Bay

Similarly, the entrance to the Morro Bay National Estuary lies 2.8 km south of the discharge and direct seawater exchange between the discharge point and the Bay is restricted by the southerly orientation of the mouth of the Bay, and by the presence of Morro Rock. Morro Rock is the largest physiographic feature of the adjacent coastline and extends into Estero Bay approximately 2 km south of the point of discharge (Figure 1). Its presence further restricts the direct exchange of seawater between the discharge point and the Bay.

Near the diffuser, prevailing currents generally follow bathymetric contours, which parallel the north-south trend of the adjacent coastline. Because of the rapid initial mixing achieved within 15 m of the diffuser structure, impingement of unmixed effluent onto the adjacent coastline 827 m away is highly unlikely. Nevertheless, water samples are regularly collected along the shoreline at the surfzone sampling stations shown in Figure 1. These surfzone samples are analyzed for total and fecal coliform levels. Results of these analyses are reported in monthly operational summaries and in annual reports. The instances of elevated beach coliform levels that are occasionally observed have resulted from onshore non-point sources rather than the discharge of disinfected wastewater from the MBCSD outfall (MRS 2000, 2001, 2002, 2003, 2004, 2005, 2006, 2007).

As shown in Figure 2, the water-sampling design consists of 16 fixed offshore stations located within 100 m of the outfall diffuser structure. The target locations of the 16 offshore sampling stations are indicated by the red ⊙ symbols in the Figure. The stations are situated at three distances relative to the center of the diffuser structure in order to capture any discharge-related trends in seawater properties. Six of the stations lie along a north-south axis at the same water depth (15.2 m) as the center of the diffuser. Stations 3 and 4 are positioned at the upcoast and downcoast boundaries of the ZID, at a distance of 15 m from the closest diffuser ports (Table 1). Stations 2 and 5 are located at nearfield distances (60 m) from the diffuser centroid. Stations 1 and 6 represent midfield stations, and are situated 100 m upcoast and downcoast of the centroid. Depending on the direction of the local oceanic currents at the time of sampling, one or more of these stations could conceivably be influenced by the discharge. Under those circumstances, the midfield station on the opposite side of the diffuser can act as a reference station. Comparisons of water properties at these antipodal stations quantify departures from ambient seawater properties so that compliance with the NPDES discharge permit can be evaluated.

Table 1. Description of Receiving-Water Monitoring Stations

Station	Description	Latitude	Longitude	Closest Approach Distance[1] (m)	Center Distance[2] (m)
1	Upcoast Midfield	35° 23.253' N	120° 52.504' W	88.4	100
2	Upcoast Nearfield	35° 23.231' N	120° 52.504' W	49.4	60
3	Upcoast ZID	35° 23.210' N	120° 52.504' W	15.0	20
4	Downcoast ZID	35° 23.188' N	120° 52.504' W	15.0	20
5	Downcoast Nearfield	35° 23.167' N	120° 52.504' W	49.4	60
6	Downcoast Midfield	35° 23.145' N	120° 52.504' W	88.4	100
7	Offshore Midfield	35° 23.199' N	120° 52.570' W	85.8	100
8	Offshore Nearfield	35° 23.199' N	120° 52.544' W	46.7	60
9	Offshore ZID	35° 23.199' N	120° 52.519' W	15.0	23
10	Shoreward ZID	35° 23.199' N	120° 52.489' W	15.0	23
11	Shoreward Nearfield	35° 23.199' N	120° 52.464' W	46.7	60
12	Shoreward Midfield	35° 23.199' N	120° 52.438' W	85.8	100
13	Southwest Nearfield	35° 23.176' N	120° 52.532' W	59.8	60
14	Northwest Nearfield	35° 23.222' N	120° 52.532' W	40.2	60
15	Northeast Nearfield	35° 23.222' N	120° 52.476' W	59.8	60
16	Southeast Nearfield	35° 23.176' N	120° 52.476' W	40.2	60

[1] Distance to the closest open diffuser port.
[2] Distance to the center of open diffuser section.

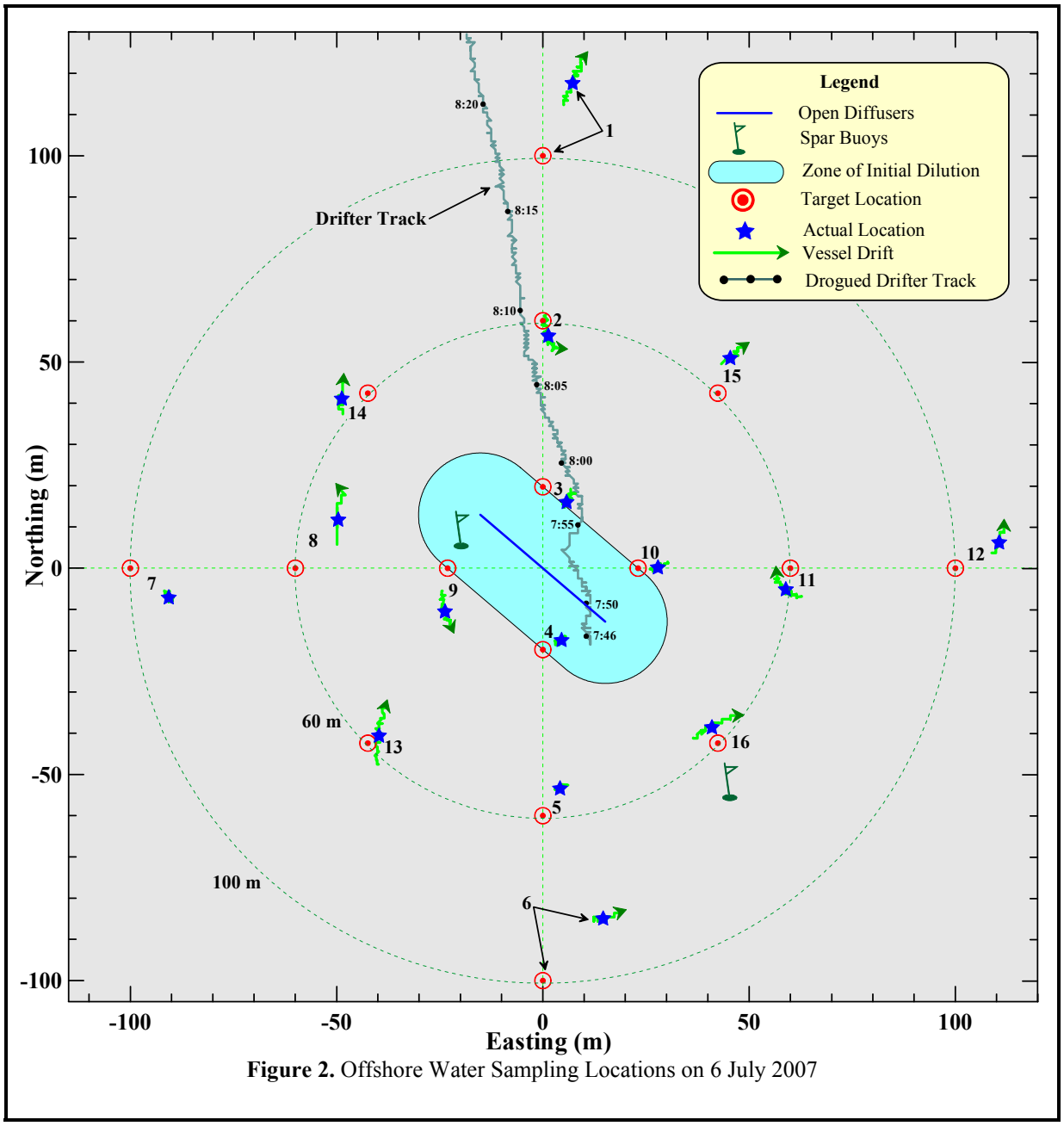

Figure 2. Offshore Water Sampling Locations on 6 July 2007

Six other stations (7 through 12) are aligned along a cross-shore transect in a pattern matching that of the along-shore transect. The remaining four stations (13 through 16) measure the nearfield influence of effluent transported by ocean currents flowing at oblique angles to the bathymetry.

An important consideration in the assessment of wastewater dispersion close to the discharge is the finite size of the diffuser. Although the discharge is considered a '*point source*' for modeling and regulatory purposes, it does not occur at a point of infinitesimal size. Instead, the discharge is distributed along a 42 m section of the seafloor. Because of this distributed discharge, the amount of wastewater dispersion at a given point in the water column is dictated by its distance to the closest diffuser port, rather than its

distance to the center of the diffuser structure. The '*closest approach*' distance can be considerably less than the centerline distance normally cited in modeling studies (Table 1).

Another important consideration for compliance evaluation is the ability to determine the actual location of the measurements. The ability to discern small spatial separations among stations within the compact sampling pattern specified in the current permit became feasible only after the advent of DGPS. The accuracy of traditional navigation systems such as LORAN or standard GPS is typically ±15 m, a span equal to half the total width of the ZID itself. Prior to 2 May 2000, standard commercial GPS receivers were not allowed to be perfectly accurate by law; and a built-in error system called Selective Availability (SA) was encoded into GPS transmissions. SA could introduce a misreading of up to 100 m, although it altered most measurements by less than 30 m. After May 2000, SA was turned off, and the accuracy of standard GPS receivers improved substantially, with horizontal position errors that are now typically less than 10 m.

Even so, extreme atmospheric conditions and physiographic obstructions can still cause satellite signals to bounce around, leading to errors in position beyond those that were previously introduced by SA. These other errors are greatly reduced with the Differential GPS (DGPS) system that was first implemented by the U.S. Coast Guard to enhance offshore navigation. DGPS incorporates a second signal from a nearby, land-based beacon. Because the beacon is fixed at a known location, the position error in the reading from the GPS satellites can be precisely calculated at any given time. This correction is continuously transmitted to the DGPS receiver onboard the survey vessel and provides an extremely stable and accurate offshore navigational reading, typically with position errors of less than 2 m.

At the beginning of 1998, the survey vessel F/V *Bonnie Marietta* was fitted with a Furuno™ GPS 30 and FBX2 differential beacon receiver. This navigational system was used on 29 July 1998 to precisely locate the position of the open section of the diffuser structure (MRS 1998b) and establish the new target locations for the receiving-water monitoring stations shown in Figure 2 and listed in Table 1. The survey vessel is now fitted with two independent DGPS receivers to allow access to two separate land-based beacons for navigational intercomparison, which ensures extremely accurate and uninterrupted navigational reports.

Frequent DGPS navigational reports allow precise determination of sampling locations during the vertical CTD profiling at individual stations. Knowledge of the precise location of the actual sampling measurements relative to the diffuser position is crucial for accurate interpretation of the water-property fields. During any given survey, the actual sampling locations do not coincide with the exact target coordinates listed in Table 1. Winds, waves, and currents induce offsets during sampling. Equally important are the offsets caused by the residual momentum of the survey vessel as it approaches the target locations. Using DGPS, these offsets can be resolved and the vessel location can be precisely tracked throughout sampling at each station. This is an important consideration because vertical profiling conducted at an individual station can cover a large horizontal distance relative to the ZID.

The magnitude of the horizontal drift that occurred at each of the stations during the July 2007 survey is apparent from the length of the green tracklines in Figure 2. These tracklines trace the horizontal location of the CTD instrument package as it is lowered to the seafloor. Their lengths reflect the station-keeping difficulty experienced during the July 2007 survey. During the time it took the CTD to traverse the water column to the seafloor, which averaged 1 min 05 s, the instrument package moved as much as 13.8 m laterally. Overall, however, drift averaged 7.3 m during the survey. This amount of drift is fairly typical of most surveys.

The CTD trajectories reflect the complex interaction between surface currents, wind forces, and residual momentum as the vessel approached each station. Winds can move the vessel to a greater degree than current flow. However, as summarized in Table B-8, winds were light and variable during the survey. As a result, their influence was minimal compared to the northward drift induced by the prevailing current. As shown by the green tracklines in Figure 2, the drift at many of the stations had a northward component. At Stations 2 and 9, the apparent southward drift of the CTD was induced by residual momentum left after the vessel approached the station from the north. The influence of vessel momentum was apparent in the vessel tracklines recorded before each downcast was conducted. Although these portions of vessel tracks are not shown in Figure 2, the approach directions were consistent with that of the vessel drift recorded throughout each CTD cast.

Although small compared to the survey vessel's length, the magnitude of CTD drift complicated the assessment of compliance with discharge limitations at stations close to the diffuser structure. Receiving-water limitations specified in the COP only apply to measurements recorded beyond the ZID boundary. Within the ZID, rapid turbulent mixing associated with the momentum of the effluent jet and the rise of the buoyant plume is expected, and the limitations apply to conditions after this initial mixing is complete. Specifically, during the July 2007 survey, the vertical profile at Station 3 traversed the boundary of the ZID (Figure 2). Thus, strictly speaking, only a portion of the data recorded during this cast was subject to the receiving-water limitations specified in the NPDES discharge permit. Additionally, none of the measurements recorded at Station 4 were subject to the limitations because the CTD was well within the ZID boundary throughout the entire vertical cast at that station.

Compliance assessments notwithstanding, measurements recorded close to the diffuser structure within the ZID lend valuable insight into the outfall's effectiveness at dispersing wastewater during the July 2007 survey. Damaged or broken diffuser ports would be reflected by low dilution rates and measurements of concentrated effluent throughout ZID. Without measurements recorded within the ZID, the discharge plume might go undetected. This was the case in nearly every water-quality survey conducted prior to 1999, before the denser sampling pattern that is now in use was instituted.

Surveys prior to 1999 also predated the advent of DGPS. Consequently, the 7.3 m average drift experienced during sampling at individual stations in the July 2007 survey would not have been resolved with the navigation available prior to 1999. In fact, before 1999 sampling was presumed to occur at a single, imprecisely determined, horizontal location near each station. Federal and State reporting of monitoring data still depends on identification of a single position for all of the CTD data collected at a particular station. Thus, for regulatory reporting, and for historical consistency with past surveys, a single sampling location was also reported for each station during the July 2007 survey. These positions were based on the average locations shown for each station by the blue stars in Figure 2. The average positions are also listed in Table 2, along with their distance from the diffuser structure. However, based on the foregoing discussion, the distance between the average station position and the ZID does not imply that all the measurements at that station were subject to the receiving-water objectives in the discharge permit. For example, the 16 m closest-approach distance specified for Station 3 would suggest that all of the data at that station were collected outside of the ZID. In reality, as shown by the green trackline in Figure 2, the near-surface measurements at Station 3 were recorded within the ZID, where water-quality limitations do not apply.

Table 2. Average Coordinates of Vertical Profiles during the July 2007 Survey

	Time (PDT)				Closest Approach	
Station	**Downcast**	**Upcast**	**Latitude**	**Longitude**	**Range[1](m)**	**Bearing[2](°T)**
1	7:58:29	7:59:50	35° 23.263' N	120° 52.499' W	107.2	12
2	8:02:20	8:03:27	35° 23.230' N	120° 52.503' W	46.6	21
3	8:06:03	8:07:11	35° 23.208' N	120° 52.500' W	**16.0[3]**	41
4	8:10:45	8:11:44	35° 23.190' N	120° 52.501' W	**10.2[4]**	221
5	8:14:58	8:15:59	35° 23.170' N	120° 52.501' W	41.8	195
6	8:19:49	8:20:51	35° 23.153' N	120° 52.494' W	71.8	180
7	8:44:47	8:46:04	35° 23.195' N	120° 52.564' W	78.1	255
8	8:41:36	8:42:40	35° 23.205' N	120° 52.537' W	34.5	268
9	8:37:34	8:38:33	35° 23.193' N	120° 52.520' W	23.3	221
10	8:34:06	8:35:09	35° 23.199' N	120° 52.486' W	18.4	44
11	8:30:46	8:31:55	35° 23.196' N	120° 52.465' W	44.5	80
12	8:28:01	8:28:50	35° 23.202' N	120° 52.431' W	97.4	79
13	8:57:00	8:58:04	35° 23.177' N	120° 52.530' W	56.6	221
14	8:48:27	8:49:39	35° 23.221' N	120° 52.536' W	43.9	310
15	8:52:06	8:53:10	35° 23.227' N	120° 52.474' W	68.3	41
16	8:23:59	8:25:05	35° 23.178' N	120° 52.477' W	36.3	135

[1] Distance from the closest open diffuser port to the average station position. Stations with some observations collected within the ZID are shown in bold.

[2] Direction measured clockwise in degrees from true north from the closest diffuser port to the average sampling location.

[3] Portions of the CTD (Conductivity-Temperature-Depth) cast were within the ZID boundary.

[4] All of the CTD cast was within the ZID boundary.

A satellite-tracked drifter documented the prevailing northward flow during the July 2007 survey. As in past reports, its trajectory is shown by the grey line with black dots in Figure 2. This drifter is designed to track the subsurface current, with little influence from the wind. Each dot along the drifter trackline represents a time span of five minutes. The drogued drifter was deployed near Station 4 at 07:46 PDT. The drifter was recovered an hour and sixteen minutes later, at 09:02 PDT. In contrast to most other surveys, the moderate northward current rapidly carried the drifter out of the survey area. Its subsequent movement is presented in Figure 3. The trajectory shows, that throughout its deployment, the drifter's movement was comparatively constant in both speed and direction, although a weak westward flow component developed after 08:00 PDT, perhaps in response to the change in tidal flow (Figure 4). During its deployment, the drifter traversed 391 m toward the north northwest (352°T) at an average speed of 8.6 cm/s or 0.17 knots.

The northward flow that was measured by the drogued drifter was not consistent with the outgoing (ebb) tide that prevailed during the survey (Figure 4). In the absence of external influences, an ebb tide normally induces a weak southwestward flow in the survey region. However, the flow is more often influenced by external processes, such as wind-generated upwelling or by passing offshore eddies. Although upwelling prevailed at the time of the survey, it normally induces a weak flow to the south. Figure 5 shows that unusually intense upwelling conditions began in February 2007, and continued steadily through at least early August, encompassing the July 2007 survey. Upwelling in prior years started later and was interrupted by periods of reduced upwelling. Evidence of intense upwelling during the July 2007 survey is apparent in the satellite image on the cover of this report. The image was recorded six days after the survey when skies were clear enough for sea-surface temperatures to be measured by infrared sensors on one of NOAA's polar orbiting satellites.

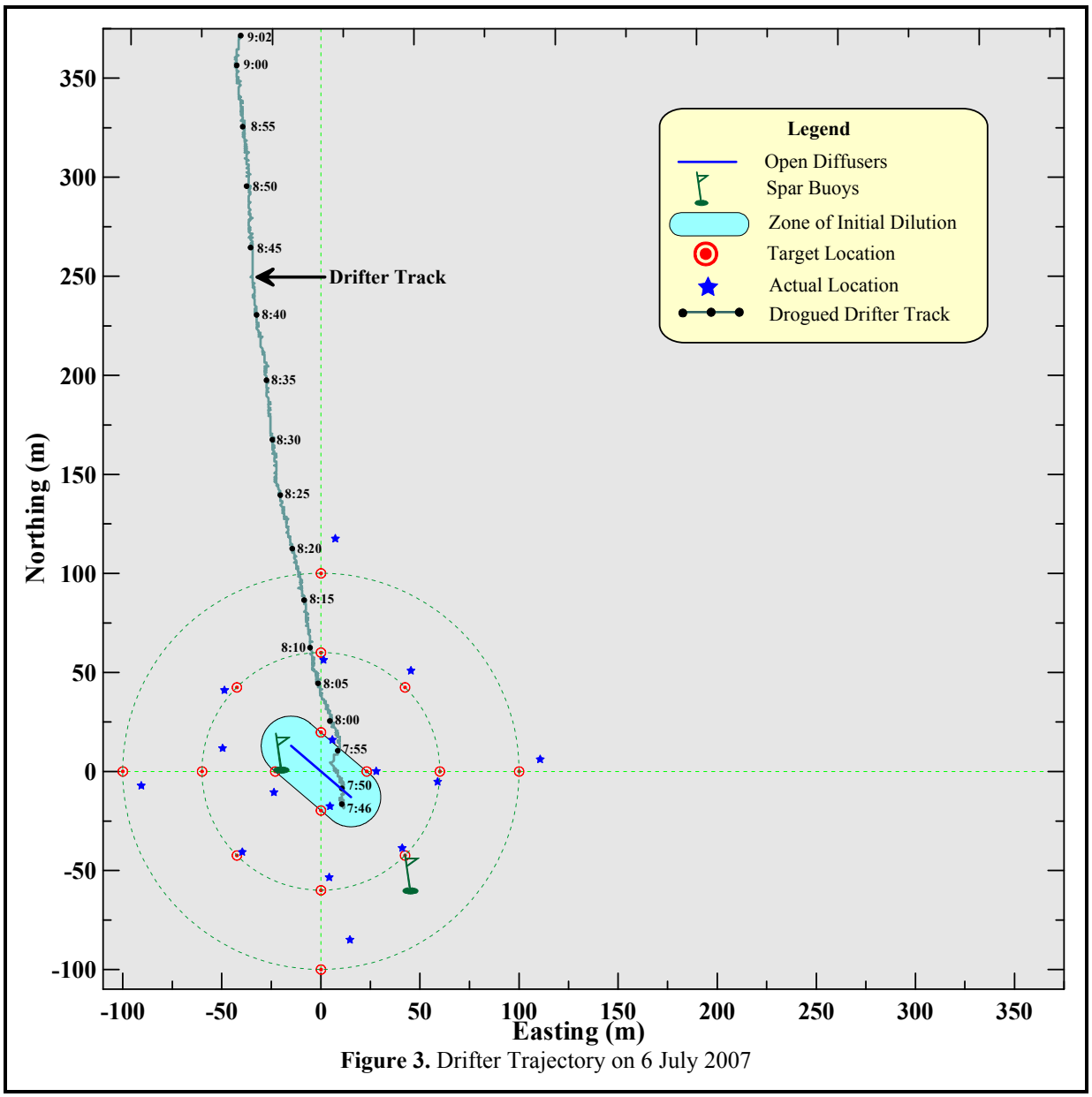

Figure 3. Drifter Trajectory on 6 July 2007

The intense upwelling that occurred around the time of the July 2007 survey was responsible for the strong water-column stratification that is evident in the vertical profiles collected with the CTD (Figures A-1 through A-3 in Appendix A). Figure 5 shows that the upwelling season normally begins sometime during late March and or early April when there is a "spring transition" to more persistent southward-directed winds along the Central California Coast. This transition is marked by the stabilization of a high atmospheric pressure field over the northeastern Pacific Ocean. Clockwise winds around this pressure field drive the prevailing northwesterly winds along the Central Coast. These prevailing winds move surface waters southward and offshore. To replace these coastal surface waters, deep, cool, nutrient-rich waters upwell near the coast.

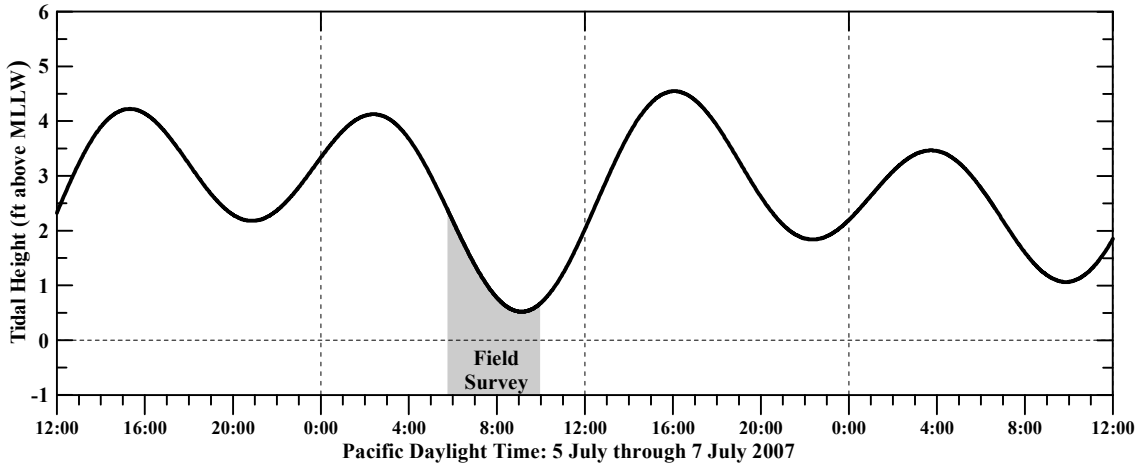

Figure 4. Estero Bay Tidal Level during the Field Survey of 6 July 2007

Strong southeastward winds prevailed along the central California coast throughout July, and the resulting upwelling induced markedly cooler sea surface temperatures close to the coastline. The satellite image on the cover depicts this colder water, with temperatures at or below 14°C, in dark blue and purple. The image also depicts another feature of upwelling wherein jets of cold coastal water extend offshore at major promontories, such as Point Buchon. These jets reflect the offshore transport of cold surface waters that were upwelled near the coast. Farther offshore, surface water temperatures were as much as five degrees warmer, as delineated by the areas with light green and yellow shading. The satellite image also shows that the cold upwelling-induced temperatures were also present in Estero Bay, where the July 2007 survey was conducted. However, near-surface temperatures measured by the CTD during the survey, which averaged 11.8°C (Table B-1 in Appendix B), were two degrees colder than depicted on the satellite image. This suggests that even more intense upwelling conditions prevailed during the survey than were recorded a week later by the satellite image. Figure 5 confirms that this was the case because the upwelling index sharply declined shortly after the survey.

The stratified character of the water column during summer upwelling conditions contrasts with the vertically uniform winter oceanographic conditions. During winter, intense winds generated by passing storm fronts, and large waves produced by distant Pacific storms, generally result in a well-mixed water column. Northwestward winds behind these storm fronts induce downwelling, which further deepens the mixed layer. Figure 5 shows that most of these downwelling events occur before May, at least in 2005 and 2006. Downwelling events, which are measured by negative downwelling indices, are highlighted in red in the Figure. In contrast to normal conditions, the winter months at the beginning of 2007 had only one, very minor, northwestward wind event, which was accompanied by weak downwelling.

METHODS

The 38 ft F/V *Bonnie Marietta*, owned and operated by Captain Mark Tognazzini of Morro Bay, served as the survey vessel on 6 July 2007. Dr. Douglas Coats of Marine Research Specialists (MRS) provided scientific support while Captain Mark Tognazzini supervised vessel operations and Mr. William Skok acted as marine technician. Mr. Bruce Keogh, MBCSD's Wastewater Division Manager, not only served

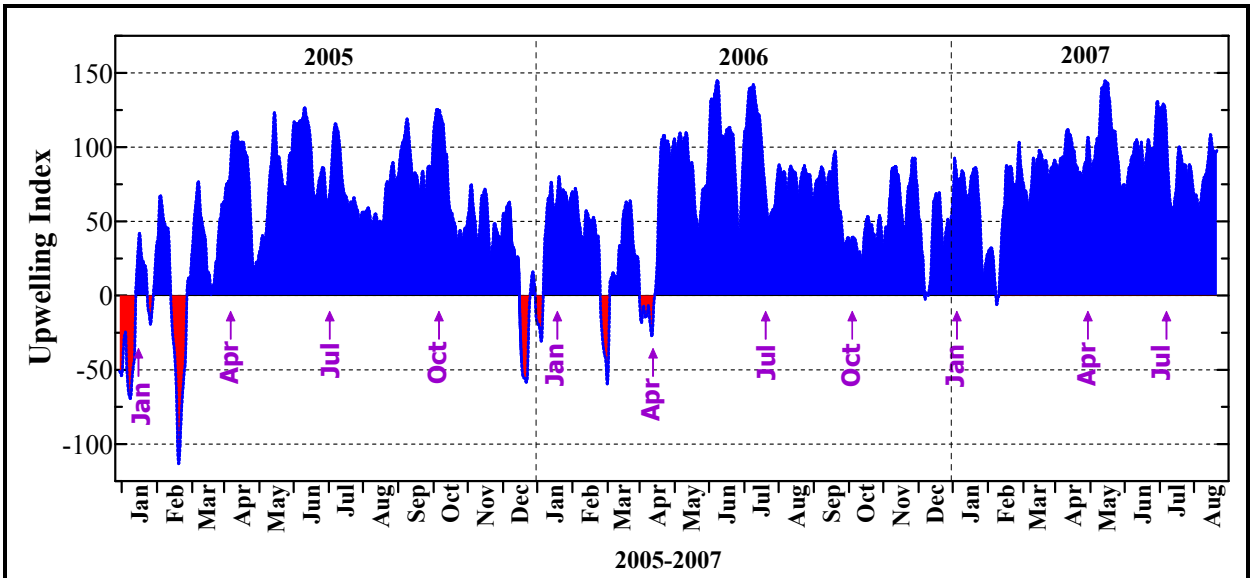

Figure 5. 30-Day Running Mean Upwelling Index ($m^3/s/100m$ of coastline) Offshore Estero Bay

as the client representative onboard the vessel during the survey, but also collected all of the auxiliary measurements of meteorological and oceanographic conditions throughout the survey. These included Secchi depth measurements and standard observations for weather, sea conditions, water clarity/coloration, and the presence of any odors, floating debris, and oil and grease that are recorded in Table B-8. Wind speeds and air temperatures were measured with a Kestrel® 2000 Thermo-Anemometer. These auxiliary observations were collected contemporaneously with the rapid water-column profiling that was conducted at each station using a CTD instrument package.

Auxiliary Measurements

At all stations, a Secchi disk was lowered through the water column to determine its depth of disappearance (Table B-8). Secchi depths provide a visual measure of near-surface turbidity or water clarity. The depth of disappearance is inversely proportional to the average amount of organic and inorganic suspended material along a line of sight in the upper water column. As such, the Secchi depth measures natural light penetration, which can be limited by increased suspended particulate loads from plankton blooms, onshore runoff, seafloor resuspension, and wastewater discharge. It is also of biological significance because the depth of the euphotic zone, where most oceanic photosynthesis occurs, extends to approximately twice the Secchi depth. Secchi depths were less than 5 m during the July 2007 survey, reflecting the presence of 10-m euphotic zone. A limited euphotic zone is typical of upwelling conditions when increased primary production, namely, increased plankton density, decreases the transmission of ambient light though the near-surface mixed layer.

However, Secchi depths are less precise than measurements recorded by the transmissometer mounted on the CTD instrument package. For example, the visibility of the disk, and hence its depth of disappearance, depends on the amount of natural light available at the time of the measurement. Thus, the Secchi depth reading can artificially change by as much as 0.5 m depending on whether the sample is taken on the sunny or shady side of the survey vessel. The Secchi depth measurements were collected in a consistent manner during the survey to minimize the effects of varying lighting conditions. Nevertheless, temporal drift in the measurements can be introduced as the sun rises in the sky, or as cloud cover changes as the survey progresses. Neither of these influences were evident during the July 2007 survey, so the Secchi

depth measurements accurately reflect general turbidity levels within the upper portion of the water column. This includes waters within a meter of the sea surface where, because of the physical size of the CTD package, the transmissometer cannot record turbidity.

During the July 2007 survey, a satellite-tracked drifter was deployed near the open section of the diffuser structure. The drifter was drogued at mid-depth (7 m) using the curtain-shade design of Davis et al (1982). In this configuration, the drifter's trajectory was largely dictated by the oceanic flow field rather than by surface winds. The times and precise positions of the drifter deployment and recovery were recorded to determine the overall strength and direction of plume transport during the July 2007 sampling effort. In addition, the July 2007 survey was the tenth MBCSD survey to record the drifter position throughout its deployment, rather than merely calculating the average flow velocity solely from the vessel position at the time of the drifter's deployment and recovery.

Instrumental Measurements

Vertical water-column profiling was conducted using an electronic instrument package equipped with a number of probes and sensors. A Sea Bird Electronics SBE-19 Seacat CTD package was used to collect profiles of conductivity, salinity, temperature, light transmittance, dissolved oxygen (DO), pH, density, and pressure at each station. A submersible pump on the CTD continuously flushed water through the conductivity cell and oxygen plenum at a constant rate, independent of the CTD's motion through the water column. After the October 2001 survey, the CTD was returned to the factory for full testing, repair, and calibration. Temporal drifts in the oxygen and alkalinity readings during the October 2001 survey indicated that the sensitivity of these probes had degraded because of an accumulation of marine growth. During the factory repair, both the pH probe and the electrolyte in the oxygen sensor were replaced. The entire CTD system was then calibrated at the factory. Upon return of the instrument, the transmissivity, dissolved oxygen, and pH sensors were recalibrated at the MRS laboratory. Calibration coefficients determined at the factory and by MRS were nearly identical, and confirmed the accuracy and stability of the refurbished sensors.

The DO and pH sensors were again returned to the factory in May 2003 and in June 2006 for testing and calibration. Because of increasing temporal drift associated with the aging DO probe, it was replaced on both occasions with a new DO probe. As is the case before all surveys, the CTD system was recalibrated at the MRS laboratory prior to the July 2007 survey. Calibration at upper-bound DO concentrations was established by immersing the CTD in an aerated, temperature-controlled calibration tank. In addition to oxygen readings at full saturation, a zero-oxygen calibration point was determined by filling the oxygen-sensor plenum with an 8% solution of sodium sulfite (Na_2SO_3). Oxygen calibration coefficients were determined by regression analysis of sensor-membrane current and temperature, as recommended by the manufacturer (SBE 1993). As with prior factory calibrations, pre-cruise calibration coefficients determined by MRS closely corresponded to those determined by the factory.

The six seawater properties that were used to assess receiving-water quality in this report were derived from the continuously recorded output from the probes and sensors on the CTD. Pressure housing limitations on the combination oxygen/pH sensor confine the CTD to depths less than 200 m (Table 3), which is well beyond the maximum depth of the deepest station in the outfall survey. The precision and accuracy of the various probes, as reported in manufacturer's specifications, are also listed in Table 3. Salinity (‰) was calculated from conductivity (Siemens/m) measurements. Density was derived from contemporaneous temperature (°C) and salinity data. It was expressed as 1000 times the specific gravity minus one, which is a unit of sigma-T (σ_t).

Table 3. Instrumental Specifications for CTD Profiler

Component	Depth[1]	Units	Range	Accuracy	Resolution
Housing	600	—	—	—	—
Pump	3400	—	—	—	—
Pressure	680	Psia	0 to 1000	± 5.0	± 0.5
Depth	—	Meters	0 to 690	± 3.0	± 0.3
Conductivity	600	Siemens/m	0 to 6.5	± 0.001	± 0.0001
Salinity	600	‰	0 to 38	± 0.006	± 0.0006
Temperature	600	ºC	–5 to 35	± 0.01	± 0.001
Transmissivity	2000	%	0 to 100	± 0.1	± 0.025
Dissolved Oxygen	200	mg/L	0 to 21.5	± 0.14	± 0.014
Acidity/Alkalinity	200	pH	0 to 14	± 0.1	± 0.006

[1] Maximum depth limit in meters

All three of these physical parameters (salinity, temperature, and density) were used to determine the lateral extent of the effluent plume. Additionally, they define the layering (vertical stratification – stability) of the receiving waters, which determines the behavior and dynamics of the wastewater as it mixes with seawater within the ZID. Data on three remaining seawater properties, consisting of light transmittance (water clarity), hydrogen-ion concentration (acidity/alkalinity – pH), and dissolved oxygen (DO), further characterize receiving waters, and were used to assess compliance with water-quality criteria. Light transmittance was measured as a percentage of the initial intensity of a transmitted beam of light detected at the opposite end of a 0.25 m path. Increased transmittance indicates increased water clarity and decreased turbidity.

During the pre-cruise calibration, coefficients for the pH (alkalinity) sensor were determined from a linear regression of output voltage after immersion in three separate buffered solutions of known pH. Buffering solutions with a pH of 4±0.01, 7±0.01, and 10±0.02 were used to bracket the range of in situ measurements. The SeaTech transmissometer was air calibrated by fitting the voltages recorded with and without blocking of the light transmission path in air, as recommended by the manufacturer (SBE 1989). Revised calibration coefficients determined prior to the survey were used in the algorithms that converted sensor voltage to engineering units when the field data were processed. Comparison with the factory calibration of the entire CTD package that was conducted in December 2001, and the more recent June 2006 replacement and calibration of the DO probe, confirmed the continued accuracy and stability of the temperature, pressure, and conductivity sensors, as well as the operational integrity of the oxygen and pH probes.

Before deployment at the initial station, the CTD was held below the sea surface for a six-minute equilibration period. Subsequently, the CTD was raised to within 1.0 m of the sea surface and profiling commenced. The CTD was lowered at a continuous rate of speed to the seafloor. Measurements at all the stations were collected during single deployment of the CTD package by towing it below the water surface while transiting between adjacent stations. Upon retrieval of the CTD, the profile data were downloaded to a portable computer and examined for completeness and range acceptability.

Temporal Trends in the pH Sensor

The pH sensor exhibited a temporal drift during the July 2007 survey. Perceptible drift in pH measurements has been consistently observed in prior water-quality surveys as the result of ongoing sensor equilibration during profiling. Prolonged exposure to the atmosphere between surveys results in the largest offsets and can also affect the dynamic range of the measurements. During past surveys, smaller equilibration offsets were also observed when the CTD was redeployed after being brought onboard to download data during the middle of the survey. Use of a single deployment during the July 2007 survey obviated the need for mid-survey adjustments for pH drift. Previous additional attempts to mitigate sensor drift have included prolonging the soak time of the CTD prior to profiling. Soak times of six minutes at the beginning of a survey were found to reduce, but not entirely eliminate sensor drift. During the July 2007 survey, a tube filled with seawater was placed around the pH sensor while in transit to the survey site to limit atmospheric exposure of the probe prior to deployment. This technique was successful at further ameliorating sensor drift.

Despite these precautions, temporal drift in the pH sensor was responsible for slight, but perceptibly lower pH measurements at stations occupied during the initial stages of the CTD deployment. Beginning with Station 1, where the offset was -0.034 pH units, equilibration-related reductions in pH became steadily smaller as the survey progressed sequentially from Station 2 (-0.033 pH) through Station 15. The magnitude of the pH offset at each station was determined by comparing pH values recorded at the seafloor with the pH measured later in the survey, when the sensor was more fully equilibrated. Removal of the artificial pH trend was important because it was large compared to reported accuracy and precision of the probe. As a result, they could potentially mask very slight discharge-related anomalies. The artificial pH reduction (-0.034 pH) at the beginning of the deployment was significantly larger than the instrumental resolution (±0.006 pH) reported by the probe manufacturer (Table 3). Before correction, equilibration-related offsets induced an artificial lateral gradient in the along-shore transect which appears in Table B-7 as an increasing seafloor pH between Stations 1 and 6. As shown in Table B-6, temporal detrending effectively removed this artificial gradient.

RESULTS

The third-quarter water-quality survey began on Friday, 6 July 2007, at 07:46 PDT with the deployment of the drogued drifter. Subsequently, all water-column measurements were collected as required by the NPDES monitoring program (Table 2 and B-9). Sunrise was at 05:54 PDT and skies were mostly clear throughout the survey, which ended at 10:00 PDT when the vessel returned to port.

Light and variable winds prevailed throughout the survey. Average wind speeds, calculated over one-minute intervals, ranged from 0.4 kt to 2.1 kt, with peak speeds ranging from 0.7 kt to 3.9 kt. Additionally, a 1 to 3 ft swell moved through the survey area from the northwest. Atmospheric visibility was greater than 2 nM along the ocean surface owing to the absence of low-lying fog. As a result, Morro Rock and the shoreline remained visible throughout the survey. Air temperatures decreased as the survey progressed. This is opposite of the trend typically observed during morning surveys, when increasing insolation from the rising sun warms the air. Instead, cool breezes from the south increased during the survey and brought a reduction in air temperature at some of the stations. The average surface seawater temperature (11.1°C) in the survey area was lower than the coldest measured air temperature (12.8°C).

The discharge plume was not visible near the sea surface at any time during the survey. Throughout the survey, there was also no visual evidence of floating particulates, oil and grease, or seawater discoloration associated with the discharge.

Beneficial Use

During the July-2007 survey, observations of beneficial use of the receiving waters of northern Estero Bay were recorded opportunistically. Southern sea otters (*Enhydra lutris nereis*) and sea lions (*Zalophus californianus*) were seen during the transit to and from the survey area, and during the survey itself. Pieces of detached floating kelp (*Nereocystis luetkeana*) were also noted in the survey area. Commercial and recreational fishing boats were observed throughout the region during the survey.

Ambient Seawater Properties

Data collected during the July 2007 survey reflected strongly stratified conditions that indicate that intense upwelling conditions were present at the time of the survey. Upwelling results in an influx of dense, cold, saline water at depth that normally leads to a sharp thermocline, halocline, and pycnocline where temperature, salinity, and density change rapidly over short vertical distances. Under heavily stratified conditions, isotherms crowd together to form a thermocline that restricts the vertical transport of the effluent plume and reduces its dispersion.

During the July 2007 survey, the vertical gradient in seawater properties was uniformly distributed over the entire depth range. In contrast to many other surveys conducted during upwelling, a single, sharp, vertically isolated change in properties was not apparent in the vertical profiles shown in Figures A-1 through A-3. Nevertheless, a large difference between surface and seafloor water properties is apparent at all stations. Temperature (red lines), DO concentrations (dark blue lines), and pH (olive lines) decreased by 2°C, 2 mg/L, 0.2 pH units with increasing depth, while density (black lines), salinity (green lines), and transmissivity (light-blue lines) increased by $0.4\sigma_t$, 0.8‰, and 6%. Except for the salinity and transmissivity fields, which were influenced by the effluent discharge, the vertical changes in seawater properties accounted for most of the variability in the seawater properties observed during the survey.

The vertical contrast in seawater properties resulted from the juxtaposition of two watermasses. Vertical mixing between the watermasses spread the vertical gradient in seawater properties across the entire water column. Nevertheless, most of the vertical profiles exhibit one or more sharp vertical changes across a narrow depth range. The sharpest change is apparent in the upper left hand frame Figure A-3. The vertical profiles at Station 13 reflect the presence of a distinct near-surface mixed layer. This relatively uniform slab of water is created by wind-induced stirring that is warmed by insolation.

The difference in seawater properties between the near-surface and deep watermasses arose because of the different processes that acted upon them. DO concentrations within the surface watermass were close to saturation from rapid equilibration with the overlying atmosphere, and from primary production (photosynthesis) by phytoplankton that thrive on the nutrients that were brought close to the surface by upwelling. The contrasting seawater characteristics of the deep watermass reflect its deeper offshore origin. Upwelling moved this cold, dense, watermass shoreward from great depths to replace the nearshore surface waters that were driven offshore by southeastward winds. Within this deep watermass, DO concentrations were comparatively low because photosynthesis was limited to the 10-m euphotic zone, and because biotic respiration and decomposition had slowly depleted oxygen levels in the watermass during the long period since its last contact with the atmosphere. Biotic respiration and

decomposition also produced dissolved CO_2 (carbonic acid), which resulted in measurably lower pH (more acidic) levels within the watermass.

The relatively higher salinity associated with the deep watermass arises from its origin in the Southern California Bight. These saline waters are carried northward below the sea surface by the Davidson Undercurrent. In contrast, surface salinity within Estero Bay is largely influenced by the diffuse southward-flowing California Current, which represents the eastern limb of the clockwise-flowing gyre that covers much of the North Pacific Ocean. Before turning south to form the California Current, sub arctic water is carried along at high latitudes where it is exposed to high precipitation and low evaporation. As a result, the waters of the California Current are characterized by a seasonably stable low salinity (32‰ to 34‰).

The cross-shore vertical section of transmissivity in the top frame of Figure A-7 depicts the intrusion and mixing processes associated with upwelling. It graphically captures the deep watermass intrusion that was in progress during the 2007 survey. The Figure delineates a tongue of less-turbid seawater in light blue just above the seafloor as it extends shoreward from Station 7 to Station 11. In the upper water column at Stations 7, 8, and 9, the less-turbid seawater from deep offshore is seen mixing with more turbid surface waters. This causes an increased light transmittance, or transmissivity, in the upper water column at those stations compared to the inshore stations. Eventually, these near-surface waters will increase in turbidity because of enhanced primary production, namely, because of plankton population growth stimulated by the availability of nutrients transported upward into the euphotic zone by upwelling.

Other processes also influenced the shape of the vertical profiles of transmissivity (light blue lines) and salinity (green lines) shown in Figure A-1 through A-3. At almost all stations, the vertical profiles of transmissivity exhibited a sharp decrease within 2 m of the seafloor. This resulted from the presence of a bottom nepheloid layer (BNL), which is a widespread phenomenon on continental shelves (Kuehl et al 1996). The increased turbidity observed within the BNL is caused by the presence of naturally occurring particulates formed from light-weight flocs of detritus. This detritus is easily suspended by oscillatory bottom currents generated by passing surface gravity waves. The vertical profiles demonstrate that the increased turbidity within the BNL along with the increased turbidity within the near-surface euphotic zone, produces a localized, turbidity minimum (transmissivity maximum) within the deep water column at most stations.

In contrast to the other water properties, some of the features in the vertical profiles of salinity (green lines) are instrumental artifacts unrelated to natural physical oceanographic processes, Often, the naturally occurring subtle increase in salinity with depth is overwhelmed by the presence of large salinity spikes in areas where localized sharp vertical changes in temperature occur. Salinity spikes are instrumental artifacts arising from the mismatch between conductivity and temperature measurements collected near sharp localized thermoclines. The spikes are evident as erroneous zigzag patterns, or localized salinity decreases that appear in conjunction with the sharp changes in temperature. Some of the larger erroneous salinity spikes also manifest themselves in the vertical density profiles (black lines). Unless properly identified, salinity spikes can be misinterpreted as a signature of the low-salinity effluent plume.

Lateral Variability

The influence of the effluent discharge can be best identified from localized anomalies in seawater properties, particularly salinity. In contrast to the isolated vertical profiles, discharge-related anomalies become especially apparent in vertical cross-sections, which highlight differences in seawater properties at adjacent stations. Accordingly, all of the cross-sections in Figures A-4 and A-5 reflect the influence of

the discharge at Station 3. The large-amplitude discharge-related reduction in salinity is especially apparent near 10 m in the top frame of Figure A-4. In, contrast, it is difficult to interpret the significance of the same salinity reduction by comparing the vertical profile in the middle-left frame of Figure A-1, with the salinity profiles at the other stations, particularly in the presence of salinity spiking.

The vertical cross-sections shown in Figures A-4 and A-5 also lend insight into the mechanism that caused the discharge-related anomaly in each seawater property. The character of the salinity and transmissivity anomalies near 10 m at Station 3, which are apparent in the top frames of Figures A-4 and A-5, are distinctly different from the anomalies in the other seawater properties that are spatially coincident. In particular, the localized reductions in salinity and transmissivity were unrelated to the ambient seawater properties at depth. They could only have been induced by the presence of dilute wastewater constituents. In contrast, the other seawater anomalies arise because of an upward excursion in the contour lines at Station 3. They have the same characteristics as ambient seawater at depth and were generated by the upward displacement of ambient seawater near the seafloor. As described above, during stratified conditions, ambient seawater properties near the seafloor differ sharply from the properties in the upper water column. These anomalies were generated when the deep ambient seawater became entrained in the discharge plume, and was displaced upward into the water column where the surrounding seawater characteristics provide a contrast.

Both the entrainment-generated and the wastewater-induced anomalies become apparent when seawater properties measured at the same depth level are compared at adjacent stations. Because of this, the analysis of lateral variability in seawater properties forms the basis for assessments of water-quality impacts in this report. In particular, the significance of each potential discharge-related anomaly was statistically evaluated by comparing its amplitude to the natural background variability. Each observation at a particular station was compared with the observations from other stations at the same depth level. Measurements recorded within 10 m of the sea surface were compared with other measurements at the same depth level below the sea surface. However, deeper measurements were compared with other measurements recorded at the same height above the sloping seafloor. These different depth references are used because deep seawater properties tend to parallel the sloping seafloor rather than the horizontal sea surface.

The statistical significance of departures from ambient seawater properties was computed from the raw CTD data listed in Tables B-1 through B-7. First, anomalies from mean conditions were computed by subtracting a particular measurement from the average of all other measurements at the same depth level, whether measured relative to the sea surface or the seafloor. Natural variability was then estimated from the standard deviation of all measurements (excluding the one in question) for a given seawater parameter (e.g., salinity). Statistically significant anomalies were those that departed from mean conditions by more than the 95% confidence interval, which is determined from the standard deviation and number of observations used to compute the average. Statistically significant departures from ambient conditions are highlighted in Tables B-1 through B-7 by bold typeface enclosed in boxes.

Only two of the six of the seawater properties exhibited statistically significant departures from mean conditions, as shown in Table B-2 (three salinity anomalies at Stations 3 and 5), and Table B-5 (one transmissivity anomaly at 9 m at Station 12). However, only one of the four significant anomalies was actually related to the discharge. The salinity anomaly at Station 3, which extends across a large vertical depth range, is clearly related to the discharge largely because it was accompanied by perceptible, but non-statistically significant anomalies in all the other seawater properties. Moreover, Station 3 was in close proximity to the outfall, and was located north of the outfall in the direct path of the prevailing flow

(Figure 4). Finally, the measured salinity within the anomaly was far lower than any salinity measured during the survey.

The same rationale can be applied to explain why the statistically significant anomalies at Stations 5 and 12 were unrelated to the discharge. First, neither station was located in the path of the plume trajectory from the diffuser structure, which is delineated by the drifter track in Figure 4. Second, Stations 5 and 12 were not in close proximity to the outfall, and the intervening Stations 4, 10, and 11, which lie closer to the outfall, did not show evidence of the discharge plume. Third, the cross-sections in Figure A-4 through Figure A-7 do not show any evidence of anomalies in other seawater properties that coincide with the salinity anomalies at Station 5, or the transmissivity anomaly at Station 12. The signature of the discharge is almost always apparent in several seawater properties at once.

Instead, the vertical cross-section of transmissivity in the top frame of Figure A-7 lends insight into the origin of the reduced transmissivity at Station 12. The deep low-turbidity watermass that was intruding shoreward had yet to reach this inshore station. Nevertheless, the statistical analysis contrasted the naturally high turbidity within mid-depth seawater at this station, with the naturally low-turbidity seawater found at the same depth level within the watermass intruding from offshore, which had reached all the other stations in the survey.

The significant salinity anomalies at Station 5 were instrumental artifacts caused by salinity spiking. Salinity spiking is a common occurrence in CTD measurements collected within upper-ocean thermoclines, and is routinely observed in MBCSD surveys conducted when the water column is well stratified (MRS, 2001, 2002, 2003, 2004, 2005, 2006, 2007). Salinity spiking occurs when the CTD package crosses a strong thermocline. Salinity is computed from conductivity and temperature probes that are physically separated from one another on the CTD. In addition, the sensors do not have the same response times so even if they are close together, they will not simultaneously report data from the same water parcel. Consequently, when encountering an abrupt temperature change, the mismatch between the conductivity and temperature readings results in erroneous spikes in the reported salinity. The sharper the thermal gradient, the larger the salinity spike.

The vertical profiles shown in the lower left frame of Figure A-1 demonstrate that this was the case for the statistically significant anomalies at Station 5. The salinity profile shown in green exhibits a classic zigzag pattern near 10 m in conjunction with several sharp changes in temperature, shown by the red line. Salinity profiles shown at most other stations exhibit similar salinity spikes, but they are not quite as large in amplitude. The increased spike amplitudes resulted from vertical oscillations in the CTD as it was lowered across a sharp thermal gradient at Station 5. The enhanced spiking was apparent in high-resolution vertical profiles of raw temperature and salinity data that were reviewed as part of an analysis of salinity spiking. The figures and data presented in this report were based on CTD measurements averaged over 0.5-m depth intervals. Although not shown here, higher-resolution profiles distinctly characterized the highly localized outliers in salinity that occurred within limited regions where there were very abrupt temperature changes. Because they were generally less than 0.5 m thick, they appear as weaker, vertically distributed features in the lower-resolution salinity profiles included in this report (green lines in Figures A-1 through A-3). Regardless of its cause, the statistically significant high-salinity anomaly at 9.5 m at Station 5 could not have been caused by the discharge of low-salinity wastewater.

Even in the absence of salinity spiking or incomplete shoreward intrusion of bottom water, the presence of statistically significant fluctuations unrelated to the discharge is expected from the nature of statistical hypothesis testing itself. From the definition of a 95% confidence level, one '*significant*' departure out of every 20 measurements should occur by chance alone. With 474 measurements examined for each of the

six parameters, it would not be surprising if a random few departed from the mean by an amount more than the 95% confidence interval. Moreover, when multiple hypotheses are being tested (*i.e.*, one for each observation), the error rate for each individual test should be adjusted to achieve the overall experimentwise error rate of 5% (95% confidence). By definition, this error rate is the probability that one or more of the hypothesis tests would incorrectly find a significant difference when none exists. Thus, without correcting for repeated hypothesis testing, the individual tests are conservative and "*significant*" departures will be found more often than if a single test were being performed at the experimentwise 95% confidence level.

Discharge-Related Perturbations

Despite the confounding influence of salinity spiking and incomplete bottom-water intrusion during the July 2007 survey, one distinct perturbation in seawater properties was unequivocally related to the discharge (Perturbation P1 in Table 4). A discharge-related perturbation is a group of anomalies in one or more seawater properties that are spatially contiguous at a particular station. The vertical distribution of seawater properties within and below the perturbation lends insight into which of two possible discharge processes was responsible for generating a particular anomaly.

Discharge-related anomalies are either induced by the presence of dilute wastewater constituents, or are generated by the upward displacement of ambient seawater that is entrained in the rising effluent plume. Wastewater-induced anomalies only occur when the contrast between the properties of wastewater and seawater are large enough to remain apparent after rapid initial dilution. Because of the large difference between wastewater and seawater salinity, wastewater-induced anomalies are usually only apparent in the salinity property. Under the right circumstances, however, wastewater-induced anomalies can also be apparent in density and transmissivity. Such was the case in the July 2007 survey (Table 4). Similarly, entrainment-generated anomalies are only apparent when the water column is stratified, and the juxtaposition of deep seawater properties carried upward in the rising effluent plume provides a contrast with shallow seawater properties. Upward transport of ambient seawater was responsible for generating the temperature, DO, and pH anomalies during the July 2007 survey (Table 4). Data collected at Station 3 during the July 2007 survey were also unusual in that they captured both a wastewater-induced, and an entrainment-generated transmissivity anomaly at different depth levels.

Table 4. Discharge-Related Water-Property Anomalies[a]

Perturbation[b]	Station	Depth Range	Depth of Extremum	Property	Magnitude	Mechanism
P1 Dilution ≥ 334:1	3	5.5 to 12.0 m	**10.0 m**	**Salinity**	**–0.101 ‰**	Effluent
		5.0 to 6.5 m	6.5 m	Density	–0.018 σ_t	Effluent
		0.0 to 11.5 m	0.0 m	Temperature	–0.60 ºC	Entrainment
		9.5 to 14.0 m	12.5 m	Transmissivity	–2.9 %	Effluent
		0.0 to 3.0 m	1.5 m	Transmissivity	2.8 %	Entrainment
		0.0 to 12.0 m	9.5 m	Dissolved Oxygen	–1.17 mg/L	Entrainment
		0.0 to 12.5 m	2.0 m	pH	–0.067	Entrainment

[a] Anomalies shown in bold type were statistically significant

[b] Perturbations are composed of a group of spatially coincident anomalies in several different seawater properties

The mechanism that produced a discharge-related anomaly is an important consideration when assessing the discharge's compliance with the receiving-water objectives of the COP, and the requirements of the NPDES permit. As indicated in Table 4, only three of the seven anomalies reflected the presence of dilute wastewater, while the anomalies in other water properties were generated by entrainment of ambient seawater within the rising effluent plume. Because the thermal, transmissivity, pH and DO anomalies reflect the properties of ambient seawater that has been displaced upward, they are not subject to water-quality restrictions that were developed to limit the discharge of wastewater contaminants.

The mechanism that generated each anomaly also lends insight into the dynamics of the effluent plume at various levels within the water column. The wastewater-induced anomalies were restricted to a limited subsurface depth range, and indicate that, at that point, the plume was continuing to undergo additional initial dilution. This is apparent from the negative density anomaly at 6.5 m which indicates that the plume was highly buoyant, and would continue to rise though the water column. The turbulence associated with the plume's rise would provide additional dilution. This is further confirmed by the classical S-shape density inversion that is apparent near 5 m at Station 3 in the bottom frame of Figure A-4. It shows that the negative density anomaly created a large, artificial inversion, wherein a buoyant parcel of water was surrounded by much denser ambient seawater. Under natural oceanic conditions, even small instabilities like this almost never occur because seawater overturn takes place rapidly. The associated turbulent mixing maintains a universally stable water column with steadily increasing density with increasing depth. Thus, an inversion such as that recorded by the density anomaly would be an extraordinarily unlikely and transient feature under natural conditions in the open ocean. It shows that the profile at Station 3 captured the plume while it was in the process of actively mixing with seawater.

In contrast to the wastewater-induced anomalies, the entrainment-generated anomalies in temperature, DO, and pH extend throughout the water column at Station 3. This broad vertical extent is apparent in the middle and bottom frames of Figure A-5, and the middle frame of A-4. The upward displacement of isopleths at Station 3 is apparent at all depth levels above 14 m, and even reach the sea surface. This demonstrates that the plume was not trapped at depth below a thermocline, and instead, had achieved maximum dilution during its turbulent rise to the sea surface. In contrast, modeling suggests that when the water column is heavily stratified, dilution is limited by a plume that becomes trapped below the sea surface. This was not the case for the July 2007 survey.

The pair of transmissivity anomalies shown in the top frame of Figure A-5 is particularly unusual. The increased transmissivity between 9.5 m and 14 m at Station 3 is delineated in the green surrounded by higher-transmissivity water delineated in blue. This slight 2.9% decrease in transmissivity was caused by the presence of dilute wastewater particulates at that location. Seawater at depth had higher transmissivity so the mid-depth anomaly could not have been generated by the upward entrainment of ambient seawater. This contrasts with the upward excursion of low transmissivity water that is apparent above the mid-depth anomaly at Station 3. This created a positive anomaly where surface waters actually had higher transmissivity than the surrounding ambient seawater. However, the increased transmissivity at the sea surface was slight (2.8%), and there was no visual signature of the plume noted at the time. Nevertheless, the 4.75 m Secchi depth measured at Station 3 was deeper than at most stations (Table 8).

Initial Dilution Computations

The amplitude of the negative salinity anomaly at Station 3 lends insight into the effectiveness of the outfall at dispersing effluent and, ultimately, compliance with the receiving-water objectives of the COP and NPDES discharge permit. The critical initial dilution applicable to the MBCSD outfall was

conservatively estimated to be 133:1 (Tetra Tech 1992). This estimate was based on worst-case modeling under highly stratified conditions where the trapping of the plume below the thermocline limited the mixing achieved during the buoyant plume's rise through the water column. The dispersion modeling determined that, after initial mixing was complete, 133 parts of ambient water would have mixed with each part of wastewater. The modeling predicted that this dilution would be achieved after the plume rose only 9 m from the seafloor, whereupon it would become trapped beneath a thermocline and spread laterally with no further substantive dilution. A 9-m rise translates into a trapping depth that is 6.4 m below the sea surface.

However, as described below, dilutions computed from the salinity anomaly observed at Station 3 during the July 2007 survey demonstrated that the effluent plume actually achieved a far higher dilution (>334:1) at depths (10 m) well below the predicted trapping depth (6.4 m). The conservative nature of the dilution ratio determined from modeling is an important consideration because it was used to specify permit limitations on chemical concentrations in wastewater discharged from the treatment plant. These end-of-pipe effluent limitations were back-calculated from the receiving-water objectives listed in the COP (SWRCB 1997) using the 133:1 dilution ratio determined from the modeling. Use of a higher critical dilution ratio would relax the stringent end-of-pipe effluent limitations that were thought to be necessary in order to meet Ocean-Plan standards.

End-of-pipe limitations on contaminant concentrations within effluent were based on the definition of dilution (Fischer et al. 1979). From the mass-balance of a conservative tracer, the concentration of a particular contaminant within effluent before discharge (C_e) can be determined from Equation 1.

$$C_e \equiv C_o + D\left(C_o - C_s\right) \qquad \textbf{Equation 1}$$

where: C_e = the concentration of a constituent in the effluent,
C_o = the concentration of the constituent in the ocean after dilution by D (*i.e.,* the COP objective),
D = the dilution ratio of the volume of seawater mixed with effluent, and
C_s = the background concentration of the constituent in ambient seawater.

By rearranging Equation 1, the actual dilution achieved by the outfall can also be determined from measured seawater anomalies. This measured dilution can then be compared with the critical dilution factor determined from modeling. Salinity is an especially useful tracer because it directly reflects the magnitude of ongoing dilution. Specifically, the salinity concentration in effluent is negligible so C_e is eliminated in Equation 1 and the dilution ratio (D) can be computed from the salinity anomaly ($A = C_o - C_s$) as:

$$D = \frac{-C_o}{\left(C_o - C_s\right)} \equiv \frac{-C_o}{A} \qquad \textbf{Equation 2}$$

where: D = the dilution ratio of the volume of seawater mixed with effluent,
C_o = the salinity of the effluent-seawater mixture after dilution by D,
C_s = the background seawater salinity (approximately 32.9‰), and
$A = C_o - C_s$ = the salinity anomaly.

The magnitude of the salinity anomaly at Station 3 (–0.101‰) was used in Equation 2 to compute the dilution level listed in the first column of Table 4 for Perturbation P1. This demonstrates that the modeled dilution factor (334:1) was significantly more conservative than the actual dilution achieved by the discharge during the July 2007 survey. Furthermore, this salinity anomaly was recorded 10 m below the

sea surface at Station 3, and the associated negative density anomaly demonstrates that additional dilution would be achieved as the effluent plume rose farther upward in the water column. Theoretically, the dilution should be lower than the model predictions at this depth because the effluent plume had not experienced as much buoyancy induced dispersion as predicted by modeling.

Even so, this dilution level is two-and-a-half times higher than the dilution predicted by conservative modeling. These dilution computations demonstrate that, during the July 2007 survey, the outfall was performing better than designed, and was rapidly diluting effluent more than 334-fold at the ZID boundary. Consequently, COP receiving-water objectives were easily met by the chemical concentration limits promulgated by the NPDES discharge permit issued to the MBCSD.

DISCUSSION

Sampling during the July 2007 survey demonstrated that the wastewater discharge was in compliance with the receiving-water limitations specified in the NPDES permit, and with the water-quality objectives of the COP (SWRCB 1997) and the Central Coast Basin Plan (RWQCB 1994). Specifically, there were no particulates of sewage origin seen floating on the ocean surface at any of the stations sampled during the July 2007 water-quality survey, and the discharge complied with all quantitative limits on seawater properties.

Although discharge-related changes in all six water properties were observed during the July 2007 survey, the changes were either not statistically significant, were measured near the boundary of the ZID before initial dilution was complete, or resulted from the displacement of ambient seawater rather than the presence of effluent constituents. Receiving-water limitations only apply to statistically significant changes caused by the presence of effluent constituents after initial dilution has been completed beyond the ZID boundary. The limitations do not apply to measurements near the ZID where discharged wastewater is still undergoing rapid initial mixing with the surrounding seawater. This was the case for the mid-depth anomalies associated with Perturbation P1. Those measurements were collected at Station 3 along the boundary of ZID as the CTD drifted into the ZID (Figure 2). The buoyant instability associated with Perturbation P1 demonstrated that the plume was continuing to undergo initial mixing at that point.

Outfall Performance

An isolated mid-depth anomaly in salinity indicated the presence of dilute wastewater at Station 3. This high-precision observation demonstrated that the diffuser structure was operating better than predicted by modeling, and that the discharged wastewater experienced high levels of dilution at depth near the ZID boundary. The amplitude of the anomaly indicates that wastewater had been diluted more than 334-fold at this location. This is more than two-and-a-half times higher than the 133:1 dilution used in the NPDES permit to establish end-of-pipe concentration limits on effluent constituents. Thus, the high dilution ratio that was determined from actual measurements during the July 2007 survey demonstrated that the outfall was performing better than expected, and that the limits on wastewater contaminant concentrations specified in the MBCSD NPDES discharge permit would easily meet the receiving-water objectives of the California Ocean Plan (COP).

NPDES Permit Limits

The seawater properties measured during the July 2007 survey were statistically evaluated for compliance with the pertinent receiving-water limitations promulgated by the NPDES discharge permit and the COP.

Specifically, the permit and COP state that the discharge shall not cause the occurrence of the following conditions.

1. *Natural light to be significantly reduced at any point outside the initial dilution zone as the result of the discharge of waste*
2. *The dissolved oxygen concentration outside the zone of initial dilution to fall below 5.0 mg/L or to be depressed more than 10 percent from that which occurs naturally*
3. *The pH outside the zone of initial dilution to be depressed below 7.0, raised above 8.3, or changed more than 0.2 units from that which occurs naturally*
4. *Temperature of the receiving water to adversely affect beneficial uses*

The COP (SWRCB 1997) further defines a '*significant*' difference as '*…a statistically significant difference in the means of two distributions of sampling results at the 95 percent confidence level.*' For each observation in Tables B-1 through B-7, the statistical significance of departures from mean conditions at a given depth level were determined with an analysis of variance that compared a single observation with the mean of a larger set of samples (Sokal and Rohlf 1997, p228; Ury 1976). Although 15 independent hypothesis tests were performed at each depth level, no Bonferroni adjustment to the error rate was included, so the tests are conservative. Specifically, Bonferroni adjustment indicates that the actual confidence level for the overall null hypothesis test for differences in properties is higher, around 99.7%, rather than the 95% level that applies to a single test. The standard deviation that was applied in the tests was determined from the entire data set to reflect the full range in ambient properties, including vertical variations.

Light Transmittance

Statistical analysis revealed significant changes in instrumentally recorded light transmittance at one of the sixteen monitoring stations during in the July 2007 survey (highlighted by bold typeface in Table B-5). Although statistically significant, the anomaly was generated by the intrusion of a deep watermass containing naturally low transmissivity that reached all of the stations, except the inshore Station 12. The contrast between the naturally more-turbid seawater at that station, and the low-turbidity water at the other stations generated the anomaly. Station 12 was far removed to the east of the outfall, and not in the path of northward plume transport. Consequently, the reduction in light transmissivity was caused by natural processes rather than "*...as a result of the discharge of waste*." Furthermore, the anomaly was observed at a depth (9 m) near the base of the 9.5 m euphotic zone. Little natural light penetrates to this depth, so the anomaly could not have caused a "*…reduction in the transmittance of natural light….*"

Dissolved Oxygen

Although it is not explicitly stated in the NPDES discharge permit, the COP specifies that the DO limitation only applies to reductions that occur "*…as a result of the discharge of oxygen demanding waste materials*." Clearly, then, the DO limitation does not apply to reductions in DO caused by the movement of ambient waters, regardless of whether or not they were induced by the physics of the discharge. Thus, the slightly reduced DO concentrations observed throughout the upper water column at Station 3, which were generated by entrainment of ambient seawater, would not be subject to the limitations for that reason alone. In addition, because the DO anomaly at Station 3 was created by the upward movement of ambient seawater that was naturally depleted in oxygen, the measured value was comparable to background concentrations observed elsewhere in the water column. Consequently, it was not found to be statistically

significant, and therefore, would not be considered *"...depressed more than 10 percent from that which occurs naturally*." Regardless of their origin or statistical significance, all of the 474 DO measurements were well above the 5-mg/L minimum specified in the Basin Plan and the NPDES discharge permit.

pH

None of the pH measurements were found to depart from mean conditions by more than the 95% confidence interval. This is true in both the raw pH data (Table B-7), and in the data corrected for sensor drift (Table B-6). Consequently, the observed pH fluctuations, including the discharge-related anomaly at Station 3 were in compliance with the discharge permit. Regardless of their lack of statistical significance or relationship to the discharge, all of the 474 pH measurements collected during the July 2007 survey complied with the numerical limits on pH deviations in the discharge permit. All of the pH measurements remained between 7.95 and 8.20 and thus complied with the lower (7.0 pH) and upper (8.3 pH) bounds on discharge-induced pH changes. Because the pH anomaly at Station 3 arose due to the upward displacement of bottom water that was naturally low in pH, none of the measurements can be considered changed by '*…more than 0.2 pH units from that which occurs naturally*.'

Temperature and Salinity

The total range in temperature of 2.0ºC across all observations was largely due to naturally occurring vertical stratification. Even if changes this large were generated by the discharge, they would be considered too small '*…to adversely affect beneficial uses*….' The observed temperature range was much less than the large-scale spatial variability in sea-surface temperature shown in the satellite image on the cover of this report. Moreover, as discussed previously, it was generated by the upward displacement of ambient seawater at depth. If it had, instead, been induced by the presence of dilute wastewater, it would have appeared as a positive (warmer) anomaly. In any regard, the slightly depressed temperature was comparable to average temperatures measured below the thermocline throughout the July 2007 survey. Accordingly, this thermal anomaly was not found to be statistically significant.

Additionally, although salinity anomalies provide the best tracer of discharged effluent, their actual amplitude (-0.101‰) during the July 2007 survey was small compared to seasonal and spatial differences in salinity that occur along the south-central California coast. For example, seasonal differences in average salinity at this location are six times higher (0.64‰). In any regard, the observed ranges in both the reported temperature (2ºC) and salinity (-0.101‰) across all data collected during the July 2007 survey were too small to be considered harmful to marine biota or deleterious to beneficial uses.

Conclusions

All of the measurements recorded during the July 2007 survey complied with the receiving-water limitations specified in the NPDES discharge permit. The discharge-related anomalies in temperature, DO, and pH that were found throughout the water column at Station 3 were caused by the upward displacement of ambient seawater and not the presence of wastewater constituents. Salinity, density, and transmissivity anomalies found at mid-depth along the ZID boundary at Station 3 were associated with the presence of dilute wastewater constituents that were continuing to undergo initial dilution. Nevertheless, measured dilution levels were two-and-a-half times larger than that predicted by modeling after completion of initial mixing. These measurements confirm that the diffuser structure and the outfall were operating better than expected from the modeling.

REFERENCES

California Department of Fish and Game (CDFG). 2000. Black Rockfish, *Sebastes melanops*, 1993-1999 Commercial Catch by Ports & Blocks. In: Volume 1, Marine Fisheries Profiles. California Department of Fish and Game, Marine Region. December 2000.

Davis, R.E., J.E. Dufour, G.J. Parks, and M.R. Perkins. 1982. Two Inexpensive Current-Following Drifters. Scripps Institution of Oceanography, University of California, San Diego, La Jolla, California. SIO Reference No. 82-28. December 1982.

Dohl, T.D., R.C. Guess, M.L. Duman, R.C. Helm. 1983. Cetaceans of central and northern California, 1980-1983: status, abundance, and distribution. Prepared for the U.S. the Department of the Interior, Minerals Management Service, Pacific OCS Region, Los Angeles, California. pp. 284.

Fischer, H.B., E.J. List, R.C.Y. Koh, J. Imberger, and N.H. Brooks. 1979. Mixing in Inland and Coastal Waters. New York: Academic Press, 483 p.

Herzing, D.L. and B.R. Mate. 1984. Gray whale migration along the Oregon coast, 1978-1981. In: M.L. Jones, S.L. Swartz, and S. Leatherwood [Eds.]. The Gray Whale, *Eschrichtius robustus*. Academic Press: Orlando, Florida. pp. 289-307.

Kuehl, S.A., C.A. Nittrouer, M.A. Allison, L. Ercilio, C. Faria, D.A. Dukat, J.M. Jaeger, T.D. Pacioni, A.G. Figueiredo, and E.C. Underkoffler 1996. Sediment deposition, accumulation, and seabed dynamics in an energetic fine-grained coastal environment. *Continental Shelf Research*, 16: 787-816.

Marine Research Specialists (MRS). 1998a. City of Morro Bay and Cayucos Sanitary District, Offshore Monitoring and Reporting Program, Water Column Sampling, March 1998 Survey. Prepared for the City of Morro Bay, CA. April 1998.

Marine Research Specialists (MRS). 1998b. City of Morro Bay and Cayucos Sanitary District, Offshore Monitoring and Reporting Program, Semiannual Benthic Sampling Report, April 1998 Survey. Prepared for the City of Morro Bay, CA. July 1998.

Marine Research Specialists (MRS). 1998c. City of Morro Bay and Cayucos Sanitary District, Offshore Monitoring and Reporting Program, Water Column Sampling, July 1998 Survey. Prepared for the City of Morro Bay, CA. August 1998.

Marine Research Specialists (MRS). 2000. City of Morro Bay and Cayucos Sanitary District, Offshore Monitoring and Reporting Program, 1999 Annual Report. Prepared for the City of Morro Bay, California. February 2000.

Marine Research Specialists (MRS). 2001. City of Morro Bay and Cayucos Sanitary District, Offshore Monitoring and Reporting Program, 2000 Annual Report. Prepared for the City of Morro Bay, California. February 2001.

Marine Research Specialists (MRS). 2002. City of Morro Bay and Cayucos Sanitary District, Offshore Monitoring and Reporting Program, 2001 Annual Report. Prepared for the City of Morro Bay, California. February 2002.

Marine Research Specialists (MRS). 2003. City of Morro Bay and Cayucos Sanitary District, Offshore Monitoring and Reporting Program, 2002 Annual Report. Prepared for the City of Morro Bay, California. February 2003.

Marine Research Specialists (MRS). 2004. City of Morro Bay and Cayucos Sanitary District, Offshore Monitoring and Reporting Program, 2003 Annual Report. Prepared for the City of Morro Bay, California. February 2004.

Marine Research Specialists (MRS). 2005. City of Morro Bay and Cayucos Sanitary District, Offshore Monitoring and Reporting Program, 2004 Annual Report. Prepared for the City of Morro Bay, California. February 2005.

Marine Research Specialists (MRS). 2006. City of Morro Bay and Cayucos Sanitary District, Offshore Monitoring and Reporting Program, 2005 Annual Report. Prepared for the City of Morro Bay, California. February 2006.

Marine Research Specialists (MRS). 2007. City of Morro Bay and Cayucos Sanitary District, Offshore Monitoring and Reporting Program, 2006 Annual Report. Prepared for the City of Morro Bay, California. February 2007.

Morro Group, Inc. 2000. MFS Globenet Corp./WorldCom Network Services Fiber Optic Cable Project Final Environmental Impact Report. SCH No. 98091053. Volume I. Submitted to: County of San Luis Obispo Department of Planning and Building. Prepared in association with Arthur D. Little, Inc. and Marine Research Specialists. January 2000.

Regional Water Quality Control Board (RWQCB) - Central Coast Region. 1994. Water Quality Control Plan (Basin Plan) Central Coast Region. Available from the RWQCB at 81 Higuera Street, Suite 200, San Luis Obispo, California. 148p. + Appendices.

Regional Water Quality Control Board (RWQCB) - Central Coast Region. 1998. Administrative Extension of Waste Discharge Requirements/National Pollution Discharge Elimination System (NPDES) CA0047881, Order 92-67. Letter to Mr. William Boucher, Director of Public Works, City of Morro Bay from Roger W. Briggs, Executive Officer. 10 April 1998.

Regional Water Quality Control Board (RWQCB) - Central Coast Region and the Environmental Protection Agency (EPA) – Region IX. 1998a. Waste Discharge Requirements (Order No. 98-15) and National Pollutant Discharge Elimination System (Permit No. CA0047881) for City of Morro bay and Cayucos Sanitary District, San Luis Obispo County. 11 December 1998.

Regional Water Quality Control Board (RWQCB) - Central Coast Region and the Environmental Protection Agency (EPA) – Region IX. 1998b. Monitoring and Reporting Program No. 98-15 for City of Morro Bay and Cayucos Sanitary District, San Luis Obispo County. 11 December 1998.

Reilly, S.B. 1984. Assessing gray whale abundance: a review. In: M.L. Jones, S.L. Swartz, and S. Leatherwood [Eds.]. The Gray Whale, *Eschrichtius robustus*. Orlando, Florida: Academic Press. pp. 203-223.

Rice, D.W., A.A. Wolman and H.W. Braham. 1984. The gray whale, *Eschrichtius robustus*. In: J.M. Briewick and H.W. Braham [Eds.]. The Status of Endangered Whales. Mar. Fish. Rev. 46(4):7-14.

Rugh, D.J. 1984. Census of gray whales at Unimak Pass, Alaska: November-December 1977-1979. In: M.L. Jones, S.L. Swartz, and S. Leatherwood. (Eds.). The Gray Whale, *Eschrichtius robustus*. Orlando, Florida: Academic Press. pp. 225-248.

Sea-Bird Electronics, Inc. (SBE) 1989. Calculation of M and B Coefficients for the Sea-Tech Transmissometer. Application Note No. 7, Revised September 1989.

Sea-Bird Electronics, Inc. (SBE) 1993. SBE 13/22/23/30 Dissolved Oxygen Sensor Calibration and Deployment. Application Note No. 13-1, rev B, Revised April 1993.

Sokal, R.R. and F.J. Rohlf. 1997. Biometry: the Principals and Practice of Statistics in Biological Research, 3rd ed. New York: W.H. Freeman and Company, 850 p.

Southern California Bight Pilot Project Field Coordination Team (SCBPPFCT). 1995. Field Operation Manual for Marine Water-Column, Benthic, and Trawl monitoring in Southern California. August 22, 1995.

State Water Resources Control Board (SWRCB). 1997. Water quality control plan, ocean waters of California, California Ocean Plan. California Environmental Protection Agency. Effective July 23, 1997.

Sund, P.N. and J.L. O'Connor. 1974. Aerial observations of gray whales during 1973. Mar. Fish. Rev. 36(4):51-55.

Tetra Tech. 1992. Technical Review City of Morro Bay, CA Section 301(h) Application for Modification of Secondary Treatment Requirements for a Discharge into Marine Waters. Prepared for the U.S. Environmental Protection Agency, Region IX, San Francisco, CA by Tetra Tech, Inc., Lafayette, CA. February 1992.

Ury, H.K. 1976. A comparison of four procedures for multiple comparisons among means (pairwise contrasts) for arbitrary sample sizes. *Technometrics*, 18: 89–97.

APPENDIX A

Water Quality Profiles and Cross Sections

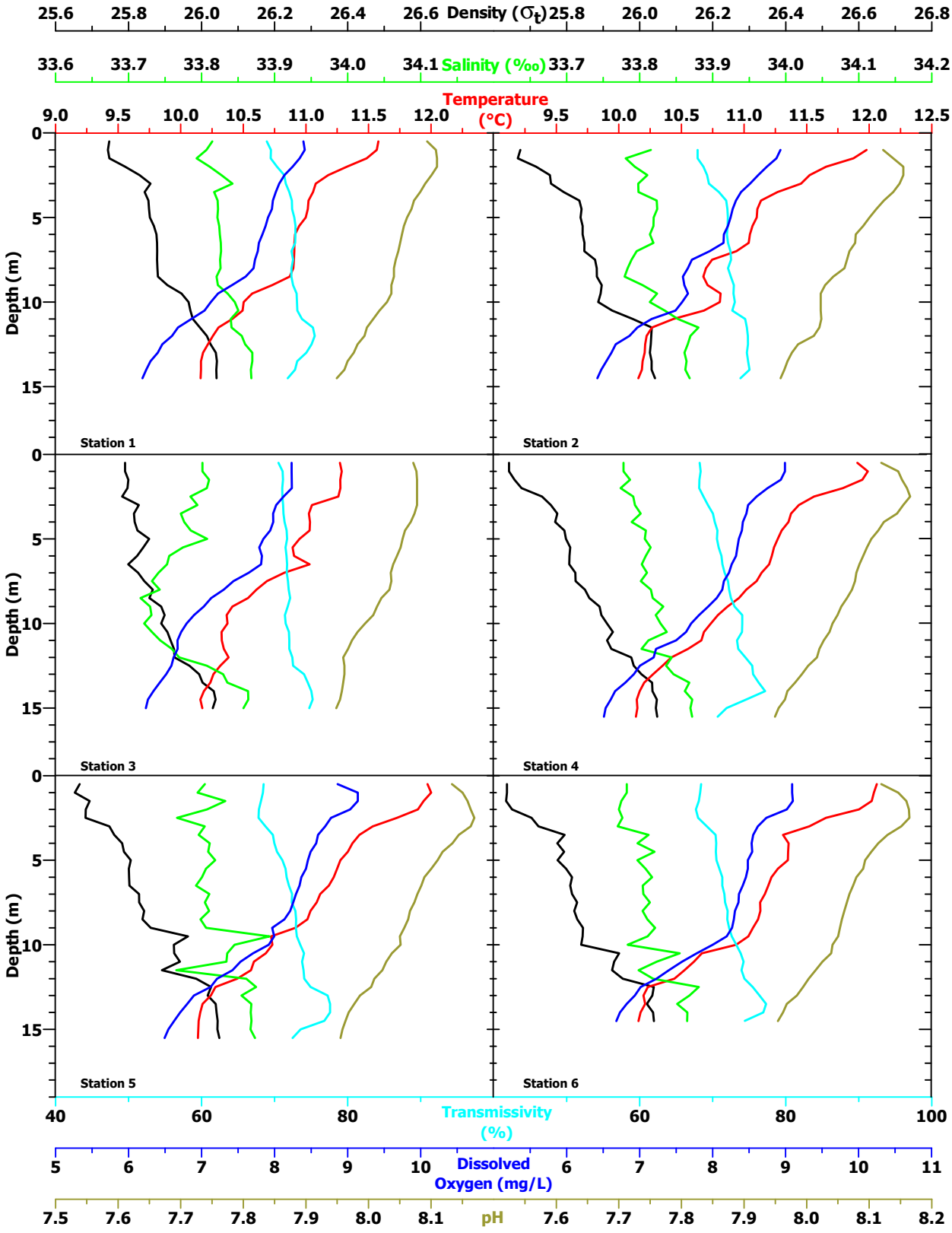

Figure A-1. Vertical Profiles of Water-Quality Parameters for Stations 1 through 6 measured on 6 July 2007

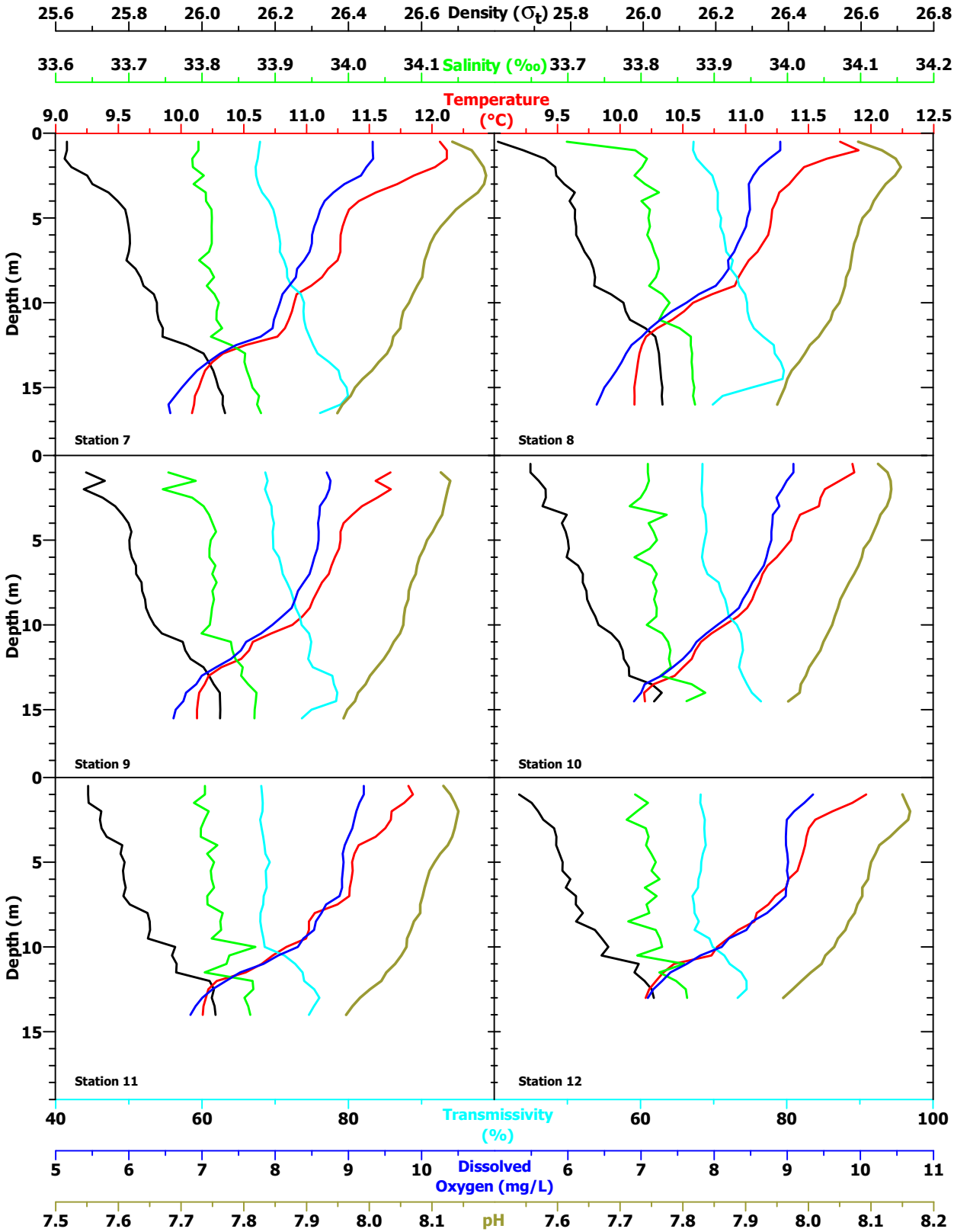

Figure A-2. Vertical Profiles of Water-Quality Parameters for Stations 7 through 12 measured on 6 July 2007

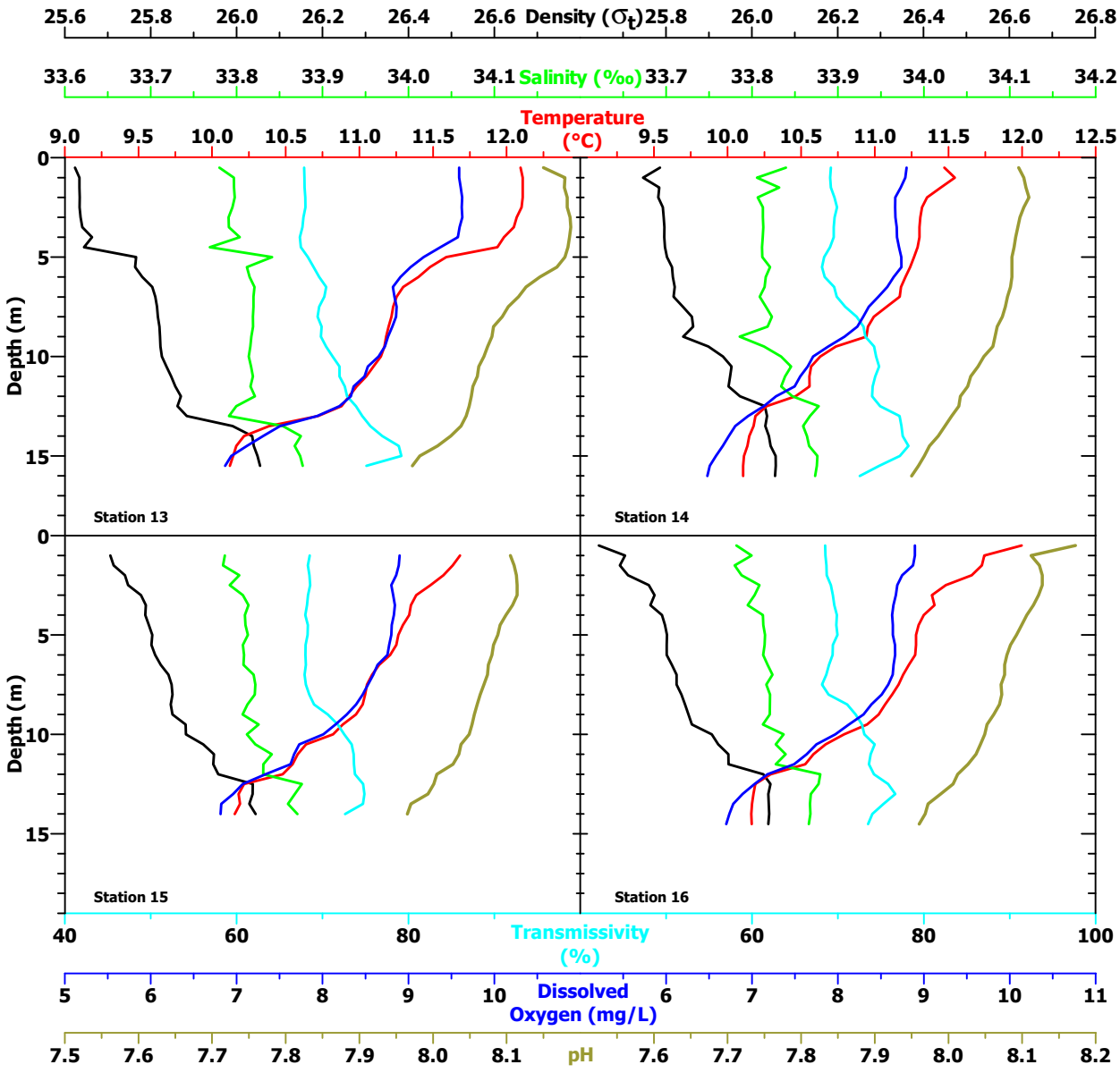

Figure A-3. Vertical Profiles of Water-Quality Parameters for Stations 13 through 16 measured on 6 July 2007

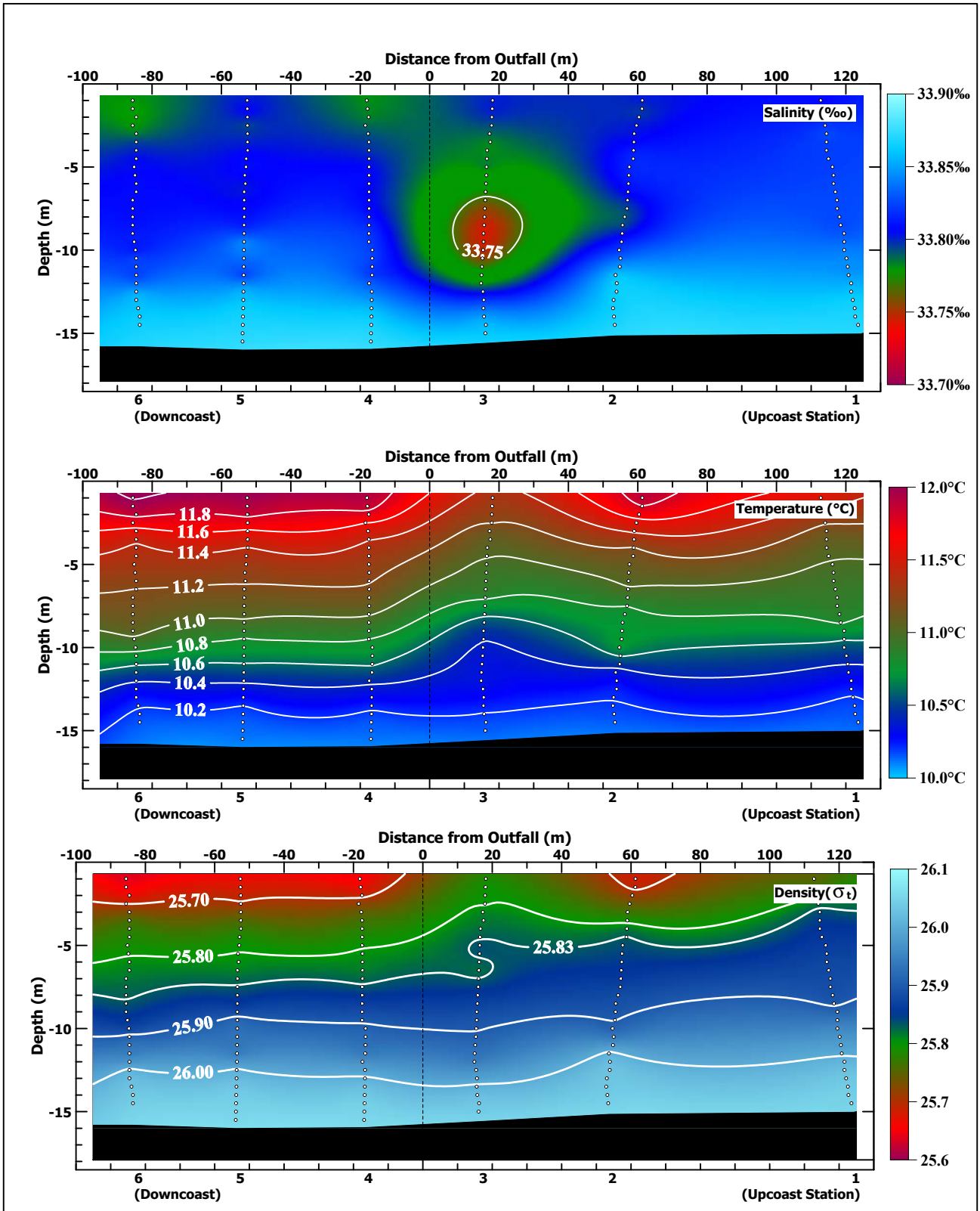

Figure A-4. Along-Shore Transects of Salinity, Temperature, and Density on 6 July 2007

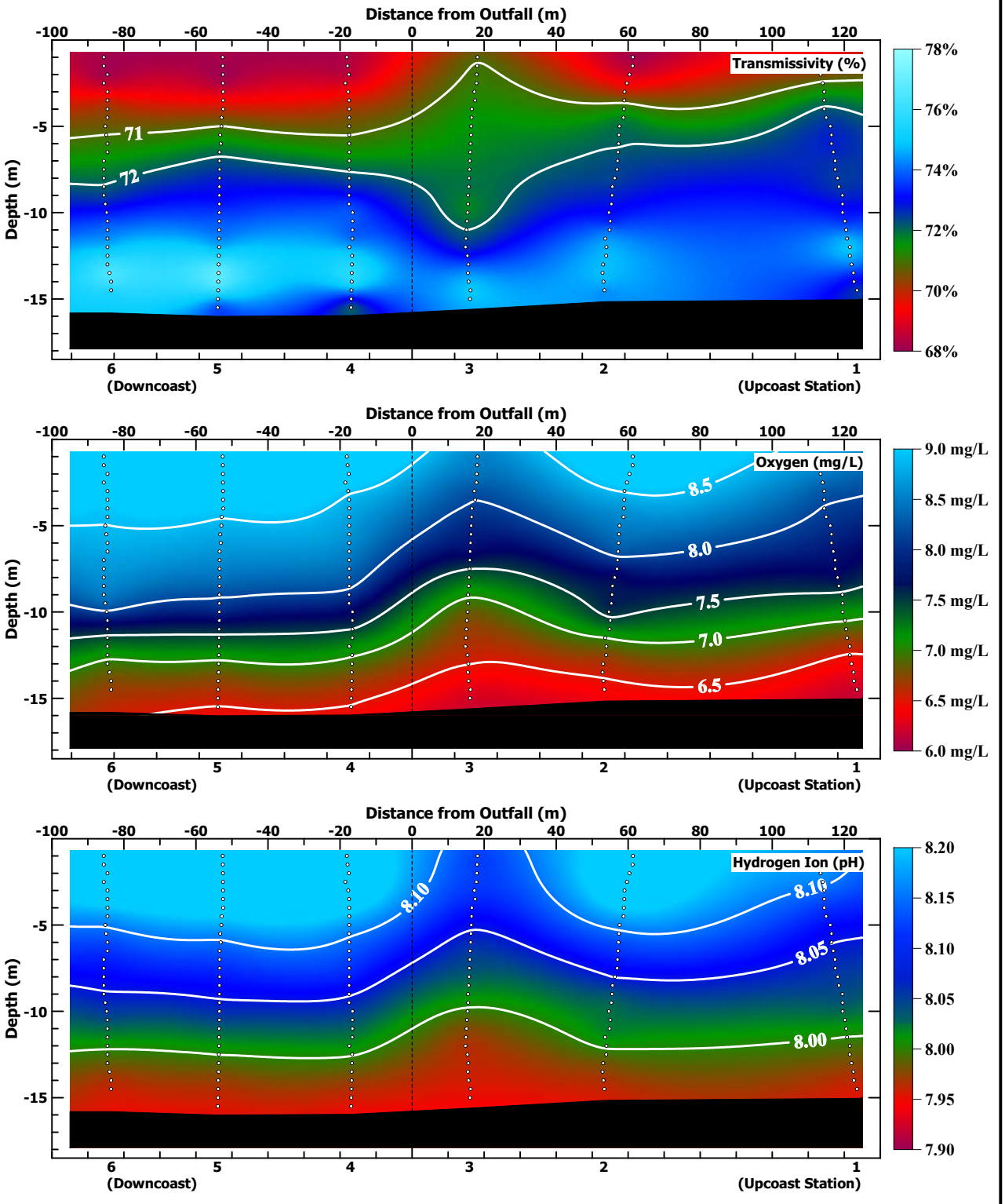

Figure A-5. Along-Shore Transects of Transmissivity, Oxygen, and pH on 6 July 2007

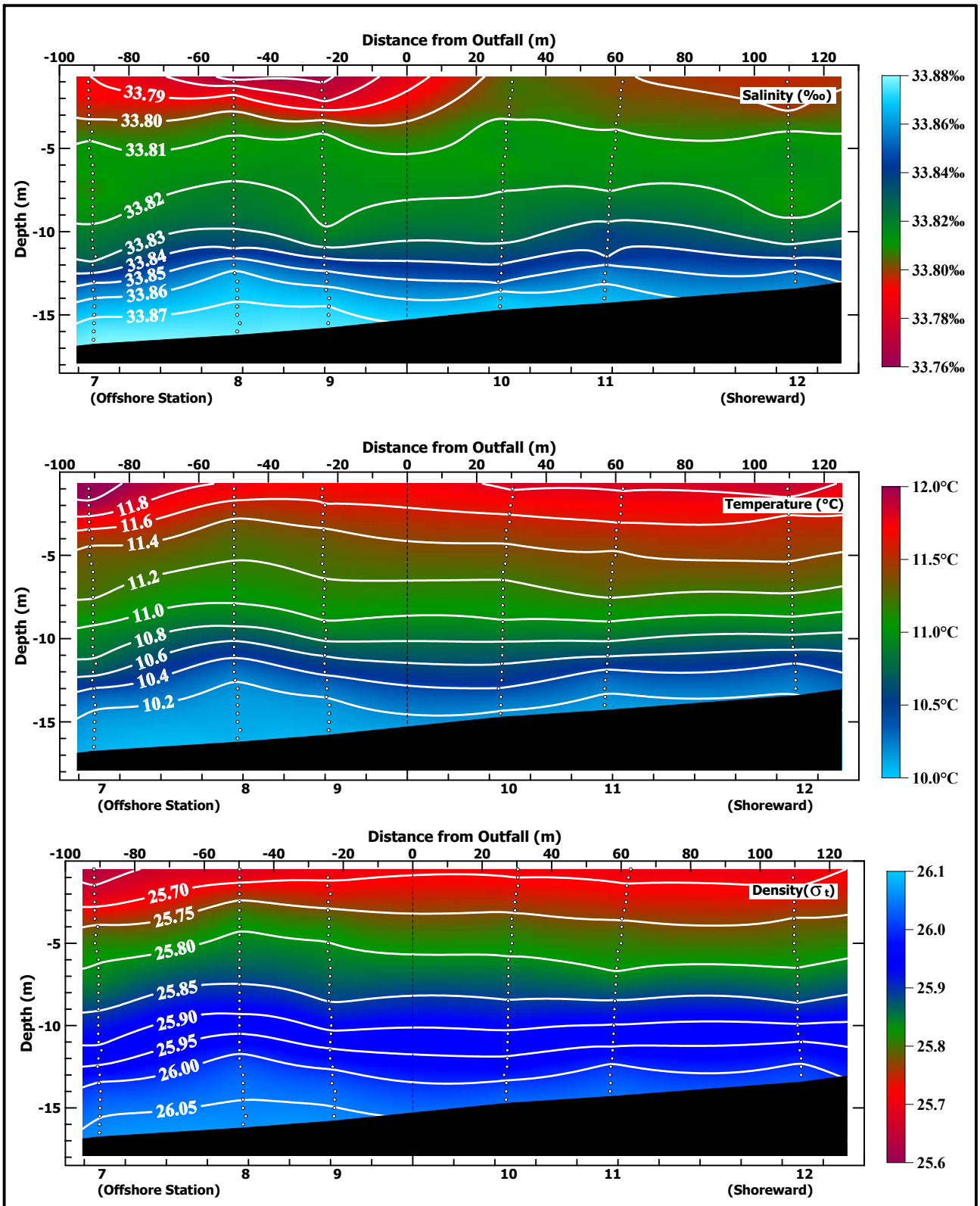

Figure A-6. Cross-Shore Transects of Salinity, Temperature, and Density on 6 July 2007

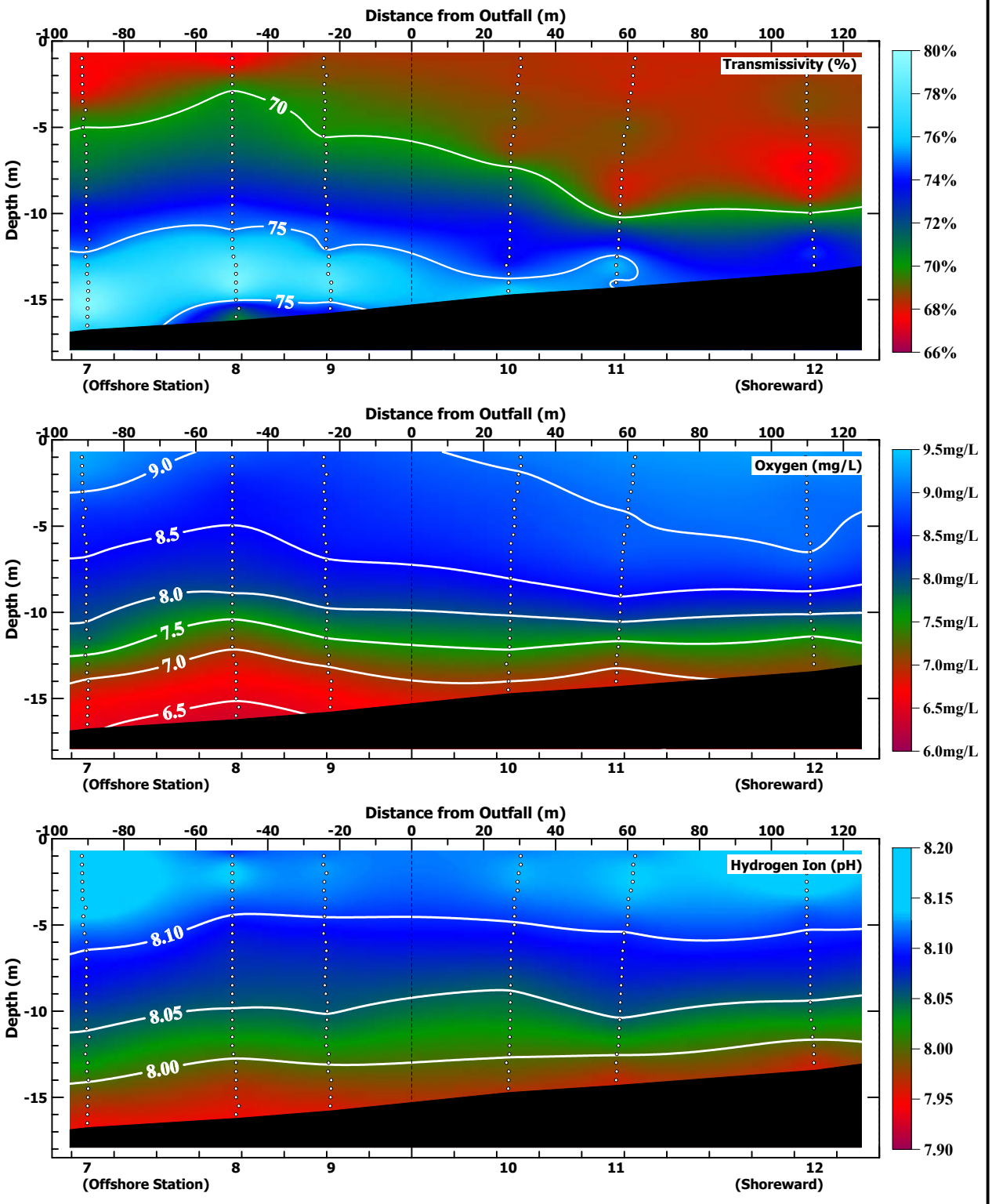

Figure A-7. Cross-Shore Transects of Transmissivity, Oxygen, and pH on 6 July 2007

APPENDIX B

Tables of Profile Data and Standard Observations

Table B-1. Seawater Temperature on 6 July 2007

	Temperature (°C)															
Depth (m)	**1**	**2**	**3**	**4**	**5**	**6**	**7**	**8**	**9**	**10**	**11**	**12**	**13**	**14**	**15**	**16**
0.5	11.58		11.27	11.91	11.97	12.06	12.06	11.75		11.85	11.81		12.09	11.47		12.00
1.0	11.57	11.98	11.29	11.99	12.00	12.04	12.12	11.90	11.67	11.87	11.85	11.96	12.11	11.54	11.68	11.74
1.5	11.49	11.87	11.27	11.95	11.94	12.02	12.12	11.65	11.55	11.75	11.78	11.85	12.11	11.45	11.63	11.73
2.0	11.33	11.66	11.28	11.79	11.89	11.92	12.02	11.47	11.67	11.63	11.68	11.69	12.11	11.36	11.57	11.66
2.5	11.18	11.52	11.26	11.56	11.73	11.65	11.86	11.40	11.56	11.60	11.67	11.56	12.10	11.32	11.48	11.48
3.0	11.08	11.45	11.05	11.44	11.53	11.52	11.72	11.35	11.44	11.58	11.63	11.50	12.07	11.31	11.39	11.39
3.5	11.06	11.27	11.02	11.38	11.43	11.31	11.55	11.27	11.36	11.43	11.55	11.49	12.05	11.30	11.35	11.40
4.0	11.02	11.14	11.03	11.36	11.37	11.36	11.42	11.24	11.30	11.40	11.42	11.48	11.98	11.30	11.34	11.33
4.5	11.02	11.11	11.03	11.30	11.34	11.35	11.34	11.21	11.27	11.38	11.38	11.46	11.94	11.29	11.30	11.30
5.0	11.00	11.10	10.95	11.27	11.28	11.35	11.31	11.21	11.27	11.36	11.36	11.44	11.59	11.27	11.26	11.28
5.5	10.95	11.07	10.89	11.24	11.25	11.27	11.29	11.20	11.26	11.31	11.37	11.41	11.48	11.24	11.25	11.28
6.0	10.91	11.05	10.91	11.22	11.22	11.22	11.27	11.18	11.23	11.25	11.36	11.34	11.40	11.21	11.21	11.27
6.5	10.91	11.04	11.03	11.20	11.18	11.19	11.27	11.14	11.20	11.17	11.34	11.32	11.30	11.18	11.13	11.23
7.0	10.91	10.94	10.83	11.14	11.11	11.17	11.27	11.09	11.18	11.13	11.34	11.24	11.25	11.17	11.09	11.19
7.5	10.90	10.75	10.69	11.10	11.09	11.13	11.25	11.03	11.12	11.11	11.25	11.18	11.23	11.08	11.05	11.16
8.0	10.90	10.70	10.60	11.02	11.04	11.13	11.17	10.98	11.09	11.08	11.07	11.09	11.22	10.99	11.04	11.12
8.5	10.87	10.67	10.54	10.96	11.01	11.11	11.12	10.94	11.05	11.05	11.02	11.07	11.20	10.95	11.02	11.07
9.0	10.73	10.71	10.41	10.87	10.92	11.07	11.04	10.91	11.03	11.01	11.02	10.94	11.18	10.94	10.98	11.03
9.5	10.57	10.81	10.37	10.79	10.72	11.03	10.92	10.73	10.97	10.94	11.00	10.86	11.17	10.74	10.89	10.95
10.0	10.50	10.81	10.37	10.74	10.73	10.94	10.90	10.58	10.89	10.84	10.84	10.77	11.15	10.63	10.82	10.79
10.5	10.49	10.68	10.33	10.68	10.68	10.66	10.88	10.51	10.72	10.73	10.73	10.73	11.10	10.57	10.64	10.67
11.0	10.41	10.44	10.33	10.66	10.59	10.60	10.86	10.42	10.57	10.64	10.64	10.43	11.05	10.56	10.58	10.58
11.5	10.30	10.26	10.34	10.55	10.56	10.52	10.83	10.30	10.54	10.60	10.52	10.34	10.98	10.56	10.55	10.53
12.0	10.26	10.22	10.38	10.42	10.45	10.44	10.77	10.21	10.48	10.57	10.28	10.29	10.93	10.46	10.48	10.29
12.5	10.22	10.21	10.32	10.35	10.28	10.23	10.51	10.17	10.32	10.50	10.22	10.23	10.88	10.26	10.22	10.19
13.0	10.18	10.21	10.26	10.27	10.24	10.20	10.33	10.15	10.22	10.44	10.20	10.20	10.72	10.19	10.18	10.18
13.5	10.16	10.19	10.24	10.20	10.17	10.21	10.25	10.14	10.19	10.27	10.18		10.39	10.18	10.19	10.17
14.0	10.16	10.18	10.19	10.17	10.16	10.17	10.19	10.13	10.14	10.19	10.17		10.22	10.15	10.16	10.16
14.5	10.16	10.16	10.16	10.14	10.14	10.16	10.16	10.12	10.13	10.20			10.16	10.14		10.16
15.0			10.17	10.15	10.14		10.14	10.11	10.13				10.14	10.11		
15.5				10.14	10.14		10.11	10.11	10.13				10.12	10.11		
16.0							10.10	10.11						10.11		
16.5							10.09									

Table B-2. Salinity[1] on 6 July 2007

	Salinity (‰)															
Depth (m)	**1**	**2**	**3**	**4**	**5**	**6**	**7**	**8**	**9**	**10**	**11**	**12**	**13**	**14**	**15**	**16**
0.5	33.815		33.801	33.778	33.805	33.782	33.795	33.699		33.809	33.804		33.780	33.839		33.782
1.0	33.807	33.815	33.801	33.778	33.795	33.782	33.795	33.792	33.754	33.809	33.804	33.792	33.797	33.806	33.786	33.799
1.5	33.793	33.781	33.810	33.787	33.833	33.775	33.787	33.808	33.792	33.811	33.789	33.810	33.797	33.832	33.784	33.780
2.0	33.811	33.793	33.807	33.774	33.807	33.772	33.788	33.802	33.746	33.807	33.809	33.795	33.798	33.807	33.803	33.788
2.5	33.827	33.811	33.785	33.791	33.766	33.776	33.803	33.791	33.787	33.799	33.804	33.780	33.795	33.813	33.792	33.809
3.0	33.842	33.798	33.794	33.794	33.804	33.770	33.789	33.806	33.802	33.785	33.799	33.807	33.791	33.813	33.807	33.803
3.5	33.817	33.798	33.772	33.801	33.796	33.812	33.805	33.825	33.810	33.835	33.798	33.810	33.791	33.813	33.814	33.795
4.0	33.822	33.823	33.776	33.789	33.811	33.797	33.806	33.801	33.814	33.810	33.821	33.807	33.804	33.812	33.810	33.813
4.5	33.823	33.824	33.785	33.809	33.809	33.820	33.813	33.812	33.819	33.817	33.807	33.814	33.769	33.812	33.810	33.813
5.0	33.822	33.819	33.808	33.807	33.819	33.797	33.814	33.810	33.812	33.822	33.817	33.820	33.841	33.812	33.813	33.815
5.5	33.824	33.819	33.775	33.815	33.806	33.808	33.813	33.812	33.810	33.812	33.812	33.814	33.812	33.821	33.807	33.815
6.0	33.825	33.814	33.756	33.808	33.801	33.817	33.813	33.809	33.810	33.791	33.813	33.825	33.815	33.816	33.809	33.813
6.5	33.826	33.819	33.753	33.803	33.792	33.804	33.813	33.815	33.818	33.814	33.817	33.805	33.821	33.815	33.808	33.818
7.0	33.827	33.796	**33.741**	33.810	33.811	33.805	33.810	33.818	33.814	33.822	33.807	33.821	33.820	33.809	33.820	33.824
7.5	33.825	33.789	**33.732**	33.802	33.805	33.814	33.796	33.823	33.820	33.816	33.808	33.808	33.820	33.816	33.822	33.817
8.0	33.826	33.784	**33.743**	33.815	33.810	33.804	33.810	33.824	33.814	33.821	33.828	33.811	33.819	33.823	33.821	33.821
8.5	33.821	33.779	**33.716**	33.818	33.799	33.811	33.817	33.820	33.816	33.818	33.825	33.783	33.819	33.818	33.813	33.821
9.0	33.822	33.804	**33.730**	33.832	33.806	33.821	33.807	33.811	33.814	33.822	33.826	33.820	33.817	33.786	33.807	33.821
9.5	33.836	33.824	**33.731**	33.822	***33.893***	33.811	33.817	33.829	33.812	33.821	33.813	33.826	33.816	33.814	33.826	33.813
10.0	33.846	33.814	**33.721**	33.829	33.845	33.784	33.823	33.839	33.811	33.808	33.873	33.829	33.814	33.834	33.812	33.837
10.5	33.850	33.834	**33.732**	33.837	33.835	33.855	33.820	33.831	33.799	33.829	33.837	33.795	33.817	33.845	33.822	33.828
11.0	33.840	33.852	**33.743**	33.812	33.834	33.823	33.820	33.825	33.840	33.837	33.834	33.859	33.819	33.838	33.841	33.839
11.5	33.841	33.881	**33.759**	33.803	**33.765**	33.799	33.828	33.853	33.842	33.840	33.804	33.825	33.816	33.834	33.831	33.828
12.0	33.855	33.870	**33.769**	33.844	33.861	33.818	33.812	33.868	33.846	33.838	33.869	33.848	33.821	33.847	33.831	33.879
12.5	33.860	33.866	33.807	33.836	33.875	33.881	33.840	33.868	33.856	33.841	33.870	33.861	33.800	33.878	33.876	33.877
13.0	33.870	33.861	33.830	33.846	33.855	33.868	33.859	33.870	33.854	33.827	33.858	33.863	33.791	33.867	33.868	33.868
13.5	33.870	33.864	33.835	33.868	33.868	33.851	33.858	33.869	33.863	33.869	33.863		33.854	33.859	33.860	33.867
14.0	33.868	33.863	33.864	33.862	33.867	33.865	33.861	33.870	33.875	33.888	33.866		33.875	33.864	33.871	33.868
14.5	33.868	33.868	33.864	33.872	33.868	33.865	33.866	33.871	33.874	33.862			33.868	33.866		33.866
15.0			33.858	33.870	33.867		33.869	33.873	33.872				33.874	33.876		
15.5				33.872	33.873		33.878	33.871	33.872				33.877	33.875		
16.0							33.875	33.874						33.873		
16.5							33.881									

[1] Values enclosed in boxes differed significantly from the mean of other salinity measurements at the same distance below the sea surface.
The thinner boxes encompass values that were significantly higher than the mean of other measurements at the same distance below the sea surface.

Table B-3. Seawater Density on 6 July 2007

	Density (sigma-t)															
Depth (m)	**1**	**2**	**3**	**4**	**5**	**6**	**7**	**8**	**9**	**10**	**11**	**12**	**13**	**14**	**15**	**16**
0.5	25.747		25.790	25.642	25.666	25.637	25.631	25.600		25.690	25.689		25.624	25.786		25.644
1.0	25.744	25.673	25.790	25.642	25.653	25.637	25.631	25.670	25.683	25.690	25.689	25.658	25.634	25.747	25.706	25.705
1.5	25.748	25.666	25.800	25.657	25.694	25.634	25.625	25.729	25.735	25.712	25.690	25.693	25.634	25.784	25.713	25.693
2.0	25.791	25.716	25.797	25.676	25.683	25.650	25.643	25.758	25.677	25.731	25.725	25.711	25.635	25.782	25.740	25.712
2.5	25.830	25.754	25.782	25.733	25.682	25.703	25.686	25.761	25.728	25.732	25.721	25.725	25.634	25.793	25.747	25.760
3.0	25.860	25.757	25.828	25.757	25.748	25.723	25.700	25.783	25.763	25.723	25.726	25.755	25.637	25.795	25.777	25.773
3.5	25.844	25.792	25.815	25.774	25.761	25.794	25.745	25.812	25.783	25.790	25.740	25.761	25.641	25.796	25.789	25.764
4.0	25.855	25.835	25.817	25.768	25.782	25.774	25.770	25.797	25.799	25.776	25.782	25.760	25.663	25.796	25.787	25.791
4.5	25.856	25.841	25.824	25.793	25.788	25.793	25.790	25.812	25.807	25.786	25.778	25.769	25.645	25.798	25.796	25.798
5.0	25.858	25.838	25.856	25.798	25.806	25.775	25.796	25.812	25.802	25.793	25.788	25.778	25.766	25.803	25.804	25.802
5.5	25.870	25.844	25.840	25.810	25.801	25.798	25.800	25.815	25.802	25.795	25.784	25.778	25.763	25.814	25.802	25.802
6.0	25.876	25.844	25.824	25.808	25.802	25.815	25.803	25.816	25.808	25.789	25.786	25.799	25.780	25.816	25.810	25.802
6.5	25.878	25.849	25.799	25.807	25.802	25.809	25.803	25.828	25.820	25.821	25.792	25.787	25.803	25.821	25.823	25.814
7.0	25.879	25.849	25.826	25.824	25.829	25.815	25.800	25.838	25.820	25.834	25.785	25.815	25.811	25.818	25.841	25.825
7.5	25.878	25.878	25.843	25.824	25.829	25.829	25.793	25.854	25.835	25.834	25.803	25.814	25.815	25.839	25.849	25.825
8.0	25.879	25.882	25.866	25.850	25.843	25.821	25.818	25.863	25.836	25.843	25.851	25.834	25.817	25.860	25.851	25.836
8.5	25.880	25.883	25.857	25.862	25.838	25.829	25.832	25.867	25.844	25.846	25.857	25.815	25.820	25.863	25.847	25.845
9.0	25.906	25.896	25.890	25.890	25.861	25.845	25.840	25.865	25.847	25.856	25.858	25.867	25.822	25.840	25.851	25.853
9.5	25.945	25.893	25.899	25.895	25.963	25.843	25.869	25.911	25.857	25.868	25.852	25.886	25.823	25.899	25.881	25.860
10.0	25.964	25.886	25.890	25.910	25.924	25.840	25.877	25.945	25.870	25.877	25.927	25.904	25.826	25.933	25.882	25.907
10.5	25.970	25.925	25.906	25.927	25.925	25.944	25.877	25.952	25.891	25.912	25.918	25.885	25.837	25.953	25.922	25.922
11.0	25.976	25.981	25.915	25.911	25.941	25.930	25.882	25.963	25.948	25.933	25.931	25.988	25.848	25.950	25.947	25.946
11.5	25.995	26.033	25.924	25.922	25.892	25.924	25.893	26.006	25.954	25.943	25.93	25.976	25.857	25.946	25.945	25.946
12.0	26.014	26.031	25.926	25.977	25.986	25.953	25.892	26.033	25.969	25.947	26.021	26.004	25.870	25.973	25.957	26.027
12.5	26.025	26.030	25.967	25.984	26.026	26.039	25.958	26.039	26.004	25.961	26.033	26.023	25.862	26.030	26.037	26.043
13.0	26.039	26.028	25.994	26.005	26.017	26.035	26.004	26.043	26.019	25.961	26.027	26.029	25.884	26.035	26.037	26.039
13.5	26.042	26.033	26.003	26.034	26.039	26.019	26.018	26.045	26.032	26.023	26.034		25.991	26.031	26.029	26.039
14.0	26.040	26.033	26.033	26.035	26.041	26.037	26.031	26.047	26.049	26.051	26.037		26.036	26.040	26.044	26.041
14.5	26.041	26.042	26.038	26.047	26.044	26.039	26.038	26.049	26.050	26.030			26.040	26.044		26.039
15.0			26.031	26.044	26.043		26.045	26.053	26.050				26.049	26.055		
15.5				26.048	26.049		26.057	26.051	26.049				26.055	26.056		
16.0							26.056	26.053						26.054		
16.5							26.063									

Table B-4. Dissolved Oxygen on 6 July 2007

	Dissolved Oxygen (mg/L)															
Depth (m)	**1**	**2**	**3**	**4**	**5**	**6**	**7**	**8**	**9**	**10**	**11**	**12**	**13**	**14**	**15**	**16**
0.5	8.39		8.23	8.99	8.86	9.09	9.33	8.90		9.08	9.21		9.59	8.80		8.89
1.0	8.41	8.93	8.23	8.99	9.14	9.09	9.33	8.90	8.70	9.08	9.21	9.35	9.59	8.78	8.90	8.89
1.5	8.34	8.87	8.24	8.94	9.14	9.10	9.34	8.76	8.76	8.99	9.15	9.23	9.61	8.73	8.89	8.87
2.0	8.25	8.74	8.24	8.75	9.04	9.02	9.25	8.62	8.74	8.93	9.11	9.10	9.63	8.67	8.86	8.75
2.5	8.13	8.63	8.12	8.60	8.77	8.74	9.17	8.54	8.69	8.85	9.08	9.00	9.62	8.67	8.80	8.69
3.0	8.06	8.51	8.02	8.49	8.69	8.62	8.95	8.48	8.61	8.89	9.05	8.99	9.63	8.67	8.82	8.67
3.5	8.02	8.39	7.98	8.46	8.59	8.56	8.80	8.48	8.61	8.80	9.00	8.98	9.59	8.68	8.84	8.65
4.0	7.98	8.32	7.98	8.42	8.57	8.54	8.68	8.49	8.59	8.80	8.95	8.98	9.58	8.69	8.83	8.63
4.5	7.96	8.27	7.94	8.40	8.49	8.54	8.62	8.49	8.60	8.78	8.92	9.00	9.37	8.71	8.80	8.64
5.0	7.91	8.25	7.85	8.36	8.46	8.48	8.58	8.46	8.59	8.78	8.94	9.01	9.18	8.74	8.80	8.64
5.5	7.88	8.21	7.79	8.34	8.43	8.48	8.53	8.44	8.58	8.74	8.92	9.00	9.02	8.74	8.77	8.66
6.0	7.83	8.16	7.83	8.32	8.37	8.46	8.50	8.38	8.54	8.72	8.91	9.02	8.91	8.65	8.76	8.67
6.5	7.78	8.15	7.82	8.26	8.34	8.41	8.50	8.32	8.50	8.68	8.91	8.99	8.82	8.57	8.64	8.65
7.0	7.77	7.96	7.65	8.22	8.29	8.36	8.47	8.28	8.47	8.60	8.88	8.98	8.84	8.47	8.59	8.64
7.5	7.73	7.72	7.44	8.15	8.26	8.35	8.40	8.19	8.39	8.52	8.70	8.86	8.86	8.36	8.53	8.58
8.0	7.71	7.66	7.30	8.13	8.21	8.31	8.30	8.20	8.31	8.47	8.63	8.72	8.86	8.29	8.47	8.51
8.5	7.60	7.59	7.13	8.06	8.13	8.29	8.28	8.12	8.27	8.39	8.56	8.52	8.81	8.23	8.39	8.39
9.0	7.42	7.61	7.03	7.94	7.97	8.27	8.19	8.02	8.23	8.34	8.53	8.44	8.76	8.08	8.28	8.30
9.5	7.23	7.66	6.90	7.82	8.00	8.19	8.10	7.79	8.10	8.20	8.38	8.20	8.72	7.89	8.15	8.13
10.0	7.13	7.58	6.80	7.71	7.92	8.00	8.07	7.62	7.96	8.05	8.31	8.10	8.65	7.71	8.01	7.97
10.5	7.04	7.49	6.72	7.64	7.71	7.78	8.03	7.42	7.81	7.89	8.04	7.81	8.53	7.65	7.73	7.75
11.0	6.86	7.16	6.67	7.50	7.53	7.58	7.98	7.27	7.60	7.76	7.84	7.63	8.49	7.56	7.67	7.63
11.5	6.68	6.97	6.67	7.22	7.42	7.40	7.97	7.12	7.53	7.68	7.52	7.40	8.36	7.50	7.63	7.49
12.0	6.59	6.86	6.62	7.19	7.21	7.23	7.80	7.01	7.40	7.57	7.33	7.29	8.33	7.28	7.34	7.18
12.5	6.46	6.67	6.59	7.00	7.12	7.01	7.47	6.87	7.19	7.44	7.14	7.17	8.20	7.14	7.07	7.03
13.0	6.40	6.61	6.52	6.92	6.90	6.93	7.25	6.80	7.00	7.28	7.00	7.10	7.94	6.95	6.96	6.89
13.5	6.30	6.55	6.43	6.80	6.80	6.82	7.09	6.74	6.92	7.05	6.91		7.50	6.80	6.82	6.78
14.0	6.24	6.48	6.34	6.66	6.71	6.73	6.93	6.66	6.78	7.00	6.84		7.31	6.73	6.81	6.74
14.5	6.19	6.42	6.27	6.60	6.63	6.68	6.83	6.59	6.74	6.91			7.12	6.66		6.70
15.0			6.24	6.53	6.55		6.73	6.50	6.64				6.94	6.58		
15.5				6.51	6.49		6.63	6.45	6.61				6.87	6.51		
16.0							6.54	6.39						6.48		
16.5							6.57									

Table B-5. Light Transmittance[1] across a 0.25-m path on 6 July 2007

	Light Transmittance (%)															
Depth (m)	**1**	**2**	**3**	**4**	**5**	**6**	**7**	**8**	**9**	**10**	**11**	**12**	**13**	**14**	**15**	**16**
0.5	68.92		70.54	68.21	68.48	68.40	67.93	67.25		68.47	68.08		67.86	69.18		68.50
1.0	69.50	67.94	71.09	68.36	68.38	68.27	67.78	67.19	68.64	68.44	68.21	68.24	67.89	69.10	68.52	68.53
1.5	69.47	67.93	71.15	68.18	68.12	68.09	67.60	67.68	68.96	68.44	68.29	68.18	67.90	69.16	68.30	68.65
2.0	70.33	68.73	71.05	68.15	67.84	67.70	67.34	68.71	68.62	68.35	68.27	68.51	67.99	69.60	68.47	68.68
2.5	71.31	69.24	71.07	68.73	67.79	68.00	67.39	69.82	69.03	68.44	67.96	68.79	68.01	69.88	68.55	69.17
3.0	71.54	69.48	71.17	69.36	68.75	69.20	67.70	70.18	69.50	68.49	68.14	68.73	67.78	69.61	68.31	69.40
3.5	72.01	70.84	71.22	70.03	69.77	70.40	68.21	70.57	69.56	68.87	68.37	68.79	67.64	69.51	68.20	69.57
4.0	72.38	71.85	71.37	70.27	69.97	70.47	69.14	70.54	69.83	68.97	68.54	68.93	67.35	69.50	68.00	69.88
4.5	72.39	72.01	71.65	70.65	70.33	70.44	69.76	70.56	69.68	69.04	68.67	68.53	67.48	69.07	68.29	69.82
5.0	72.69	72.07	71.71	70.58	71.06	70.50	70.04	71.03	69.71	68.77	69.27	68.30	68.28	68.39	68.25	69.94
5.5	72.87	72.04	71.50	70.80	71.48	70.91	70.24	70.90	69.76	68.56	68.71	68.25	68.94	68.13	68.04	69.41
6.0	72.84	71.94	71.62	71.19	71.66	71.30	70.52	71.38	70.51	68.40	68.77	67.93	69.61	68.46	68.01	69.38
6.5	72.81	72.09	71.71	71.32	71.97	71.31	70.68	71.55	70.81	68.67	68.84	67.84	70.44	69.55	68.06	68.95
7.0	72.30	72.43	71.66	71.63	72.39	71.59	70.63	71.73	71.03	69.15	68.44	67.12	70.22	69.85	67.92	68.63
7.5	72.54	72.50	71.83	72.09	72.34	71.68	71.22	72.63	71.60	70.70	68.37	67.32	69.61	70.83	68.05	68.14
8.0	72.32	72.09	71.92	72.25	72.86	72.05	71.58	72.34	72.15	71.01	67.99	67.40	69.43	72.18	68.46	68.91
8.5	72.30	72.48	72.12	72.49	72.95	71.99	71.65	73.20	72.48	71.57	67.97	67.98	69.89	72.97	69.00	71.07
9.0	72.54	72.88	71.79	73.00	72.91	72.25	72.23	73.51	72.80	71.85	68.14	**67.38**	69.82	73.19	70.60	72.06
9.5	73.00	72.85	71.42	74.04	73.04	72.62	73.51	74.30	73.36	72.07	68.40	69.42	70.41	74.21	71.76	72.78
10.0	73.07	73.04	71.50	74.04	73.52	73.23	73.95	74.57	73.61	73.17	68.56	69.86	71.17	74.44	72.54	73.08
10.5	73.10	72.66	71.96	74.02	74.03	73.83	73.87	74.63	74.62	73.74	71.27	71.46	71.98	74.80	73.38	74.27
11.0	73.74	74.44	72.02	73.33	73.76	74.23	73.94	74.91	74.93	73.89	72.74	72.19	71.97	74.32	73.63	73.81
11.5	75.25	74.67	72.01	73.49	73.97	73.95	74.20	75.52	74.77	74.00	73.74	73.76	72.59	74.03	73.64	73.60
12.0	75.49	74.82	72.42	74.48	74.08	74.34	74.69	76.78	74.50	73.69	73.96	74.49	72.85	73.98	73.77	74.19
12.5	75.07	74.84	72.53	75.40	74.92	75.47	75.19	78.23	75.14	73.46	75.32	74.50	73.90	74.90	74.73	75.83
13.0	74.35	74.67	74.03	75.52	77.27	76.42	75.80	78.36	77.80	73.97	76.05	73.28	74.64	77.17	74.86	76.67
13.5	73.10	74.85	74.55	76.29	77.60	77.31	77.37	79.16	78.03	74.56	75.28		75.55	77.39	74.70	75.30
14.0	72.79	75.04	75.04	77.16	77.59	76.94	78.67	79.62	78.49	75.24	74.62		76.94	77.52	72.64	74.02
14.5	71.81	73.81	75.21	74.58	76.82	74.42	78.95	79.44	78.32	76.45			78.86	78.20		73.50
15.0			74.75	71.89	73.56		79.77	75.20	74.97				79.18	77.20		
15.5				70.69	72.48		79.94	71.22	73.66				75.14	74.81		
16.0							78.97	69.88						72.53		
16.5							76.14									

[1] Value enclosed in the box was significantly lower than the mean of other transmissivity measurements at the same distance above the seafloor.

Table B-6. Detrended[1] pH on 6 July 2007

	Hydrogen Ion Concentration (pH)															
Depth (m)	**1**	**2**	**3**	**4**	**5**	**6**	**7**	**8**	**9**	**10**	**11**	**12**	**13**	**14**	**15**	**16**
0.5	8.094		8.072	8.119	8.133	8.119	8.132	8.079		8.111	8.118		8.150	8.095		8.172
1.0	8.108	8.122	8.077	8.146	8.150	8.146	8.163	8.117	8.114	8.126	8.129	8.150	8.179	8.102	8.105	8.112
1.5	8.110	8.138	8.078	8.152	8.158	8.159	8.173	8.139	8.129	8.131	8.136	8.156	8.178	8.105	8.110	8.123
2.0	8.110	8.154	8.078	8.160	8.163	8.163	8.182	8.147	8.125	8.132	8.142	8.162	8.182	8.109	8.113	8.127
2.5	8.101	8.154	8.078	8.165	8.169	8.164	8.186	8.138	8.122	8.130	8.139	8.159	8.182	8.102	8.114	8.127
3.0	8.091	8.148	8.078	8.154	8.163	8.151	8.183	8.123	8.119	8.125	8.136	8.144	8.186	8.097	8.114	8.122
3.5	8.083	8.138	8.074	8.144	8.144	8.129	8.173	8.113	8.116	8.115	8.132	8.130	8.187	8.094	8.108	8.115
4.0	8.073	8.123	8.068	8.123	8.134	8.114	8.155	8.104	8.108	8.110	8.125	8.113	8.185	8.091	8.099	8.106
4.5	8.069	8.111	8.059	8.114	8.118	8.103	8.138	8.098	8.101	8.104	8.113	8.107	8.183	8.089	8.091	8.099
5.0	8.062	8.100	8.055	8.103	8.110	8.093	8.126	8.086	8.092	8.098	8.104	8.100	8.179	8.086	8.088	8.092
5.5	8.057	8.090	8.052	8.096	8.100	8.090	8.114	8.081	8.087	8.088	8.096	8.097	8.168	8.086	8.082	8.084
6.0	8.054	8.078	8.046	8.090	8.089	8.079	8.104	8.078	8.080	8.085	8.092	8.095	8.145	8.086	8.080	8.079
6.5	8.051	8.077	8.040	8.084	8.084	8.074	8.097	8.073	8.076	8.080	8.088	8.086	8.126	8.084	8.075	8.076
7.0	8.048	8.068	8.036	8.079	8.078	8.068	8.093	8.070	8.074	8.073	8.085	8.086	8.116	8.080	8.074	8.076
7.5	8.044	8.064	8.037	8.077	8.073	8.064	8.088	8.068	8.067	8.065	8.081	8.078	8.102	8.077	8.069	8.071
8.0	8.041	8.060	8.034	8.072	8.066	8.060	8.086	8.066	8.063	8.058	8.081	8.074	8.094	8.073	8.064	8.072
8.5	8.041	8.042	8.021	8.064	8.063	8.056	8.084	8.060	8.062	8.051	8.071	8.064	8.082	8.066	8.060	8.069
9.0	8.037	8.029	8.014	8.055	8.057	8.053	8.076	8.058	8.057	8.047	8.066	8.059	8.080	8.063	8.056	8.061
9.5	8.037	8.022	8.008	8.049	8.050	8.050	8.069	8.054	8.055	8.042	8.060	8.047	8.074	8.060	8.053	8.052
10.0	8.030	8.022	7.995	8.041	8.051	8.041	8.063	8.049	8.054	8.038	8.059	8.041	8.069	8.048	8.049	8.049
10.5	8.018	8.022	7.983	8.036	8.037	8.039	8.054	8.039	8.049	8.031	8.051	8.027	8.062	8.040	8.038	8.043
11.0	8.008	8.023	7.974	8.027	8.028	8.025	8.051	8.035	8.039	8.024	8.041	8.021	8.060	8.030	8.035	8.037
11.5	7.998	8.020	7.968	8.020	8.022	8.014	8.049	8.025	8.032	8.019	8.027	8.004	8.054	8.026	8.027	8.026
12.0	7.994	8.011	7.960	8.016	8.009	8.003	8.038	8.016	8.023	8.010	8.019	7.989	8.052	8.016	8.005	8.012
12.5	7.983	7.986	7.962	8.002	8.004	7.994	8.035	8.002	8.012	8.001	8.001	7.975	8.049	8.014	8.001	8.006
13.0	7.977	7.976	7.962	7.992	7.986	7.984	8.028	7.994	8.001	7.996	7.985	7.960	8.045	8.004	7.993	7.989
13.5	7.967	7.969	7.960	7.981	7.977	7.968	8.015	7.985	7.994	7.988	7.973		8.038	7.995	7.970	7.972
14.0	7.962	7.964	7.958	7.969	7.968	7.962	8.004	7.973	7.982	7.986	7.963		8.024	7.986	7.965	7.968
14.5	7.950	7.958	7.955	7.965	7.963	7.954	7.989	7.966	7.977	7.968			8.006	7.974		7.960
15.0			7.949	7.955	7.958		7.977	7.962	7.965				7.982	7.967		
15.5				7.949	7.955		7.970	7.956	7.959				7.972	7.959		
16.0							7.957	7.950						7.950		
16.5							7.949									

[1] Measured pH levels were corrected for temporal drift to account for ongoing equilibration of the pH sensor.

Table B-7. Uncorrected pH on 6 July 2007

	Alkalinity (pH)															
Depth (m)	**1**	**2**	**3**	**4**	**5**	**6**	**7**	**8**	**9**	**10**	**11**	**12**	**13**	**14**	**15**	**16**
0.5	8.060		8.038	8.087	8.101	8.092	8.119	8.056		8.102	8.104		8.141	8.072		8.140
1.0	8.074	8.089	8.043	8.114	8.118	8.119	8.150	8.094	8.096	8.117	8.115	8.132	8.170	8.079	8.096	8.080
1.5	8.076	8.105	8.044	8.120	8.126	8.132	8.160	8.116	8.111	8.122	8.122	8.138	8.169	8.082	8.101	8.091
2.0	8.076	8.121	8.044	8.128	8.131	8.136	8.169	8.124	8.107	8.123	8.128	8.144	8.173	8.086	8.104	8.095
2.5	8.067	8.121	8.044	8.133	8.137	8.137	8.173	8.115	8.104	8.121	8.125	8.141	8.173	8.079	8.105	8.095
3.0	8.057	8.115	8.044	8.122	8.131	8.124	8.170	8.100	8.101	8.116	8.122	8.126	8.177	8.074	8.105	8.090
3.5	8.049	8.105	8.040	8.112	8.112	8.102	8.160	8.090	8.098	8.106	8.118	8.112	8.178	8.071	8.099	8.083
4.0	8.039	8.090	8.034	8.091	8.102	8.087	8.142	8.081	8.090	8.101	8.111	8.095	8.176	8.068	8.090	8.074
4.5	8.035	8.078	8.025	8.082	8.086	8.076	8.125	8.075	8.083	8.095	8.099	8.089	8.174	8.066	8.082	8.067
5.0	8.028	8.067	8.021	8.071	8.078	8.066	8.113	8.063	8.074	8.089	8.090	8.082	8.170	8.063	8.079	8.060
5.5	8.023	8.057	8.018	8.064	8.068	8.063	8.101	8.058	8.069	8.079	8.082	8.079	8.159	8.063	8.073	8.052
6.0	8.020	8.045	8.012	8.058	8.057	8.052	8.091	8.055	8.062	8.076	8.078	8.077	8.136	8.063	8.071	8.047
6.5	8.017	8.044	8.006	8.052	8.052	8.047	8.084	8.050	8.058	8.071	8.074	8.068	8.117	8.061	8.066	8.044
7.0	8.014	8.035	8.002	8.047	8.046	8.041	8.080	8.047	8.056	8.064	8.071	8.068	8.107	8.057	8.065	8.044
7.5	8.010	8.031	8.003	8.045	8.041	8.037	8.075	8.045	8.049	8.056	8.067	8.060	8.093	8.054	8.060	8.039
8.0	8.007	8.027	8.000	8.040	8.034	8.033	8.073	8.043	8.045	8.049	8.067	8.056	8.085	8.050	8.055	8.040
8.5	8.007	8.009	7.987	8.032	8.031	8.029	8.071	8.037	8.044	8.042	8.057	8.046	8.073	8.043	8.051	8.037
9.0	8.003	7.996	7.980	8.023	8.025	8.026	8.063	8.035	8.039	8.038	8.052	8.041	8.071	8.040	8.047	8.029
9.5	8.003	7.989	7.974	8.017	8.018	8.023	8.056	8.031	8.037	8.033	8.046	8.029	8.065	8.037	8.044	8.020
10.0	7.996	7.989	7.961	8.009	8.019	8.014	8.050	8.026	8.036	8.029	8.045	8.023	8.060	8.025	8.040	8.017
10.5	7.984	7.989	7.949	8.004	8.005	8.012	8.041	8.016	8.031	8.022	8.037	8.009	8.053	8.017	8.029	8.011
11.0	7.974	7.990	7.940	7.995	7.996	7.998	8.038	8.012	8.021	8.015	8.027	8.003	8.051	8.007	8.026	8.005
11.5	7.964	7.987	7.934	7.988	7.990	7.987	8.036	8.002	8.014	8.010	8.013	7.986	8.045	8.003	8.018	7.994
12.0	7.960	7.978	7.926	7.984	7.977	7.976	8.025	7.993	8.005	8.001	8.005	7.971	8.043	7.993	7.996	7.980
12.5	7.949	7.953	7.928	7.970	7.972	7.967	8.022	7.979	7.994	7.992	7.987	7.957	8.040	7.991	7.992	7.974
13.0	7.943	7.943	7.928	7.960	7.954	7.957	8.015	7.971	7.983	7.987	7.971	7.942	8.036	7.981	7.984	7.957
13.5	7.933	7.936	7.926	7.949	7.945	7.941	8.002	7.962	7.976	7.979	7.959		8.029	7.972	7.961	7.940
14.0	7.928	7.931	7.924	7.937	7.936	7.935	7.991	7.950	7.964	7.977	7.949		8.015	7.963	7.956	7.936
14.5	7.916	7.925	7.921	7.933	7.931	7.927	7.976	7.943	7.959	7.959			7.997	7.951		7.928
15.0			7.915	7.923	7.926		7.964	7.939	7.947				7.973	7.944		
15.5				7.917	7.923		7.957	7.933	7.941				7.963	7.936		
16.0							7.944	7.927						7.927		
16.5							7.936									

Table B-8. Ancillary Observations on 6 July 2007 during the Receiving-Water Survey

Station	Location		Diffuser Distance	Time	Air Temperature	Cloud Cover	Wind Avg	Wind Max	Wind Dir (from)	Swell Ht/Dir	Secchi Depth
	Latitude	Longitude	(m)	(PDT)	(°C)	(%)	(kt)	(kt)	(°T)	(ft/°T)	(m)
1	35° 23.262' N	120° 52.496' W	113.4	7:59:50	13.0	100	1.1	1.9	SSW	1-3/NW	4.50
2	35° 23.226' N	120° 52.497' W	44.6	8:03:27	13.4	100	1.5	1.9	WSW	1-3/NW	4.50
3	35° 23.207' N	120° 52.505' W	15.7	8:07:11	13.2	100	0.4	0.7	WSW	1-3/NW	4.75
4	35° 23.186' N	120° 52.500' W	9.7	8:11:44	13.7	100	0.8	1.1	WSW	1-3/NW	4.75
5	35° 23.166' N	120° 52.501' W	42.5	8:15:59	13.8	100	1.1	3.3	WSW	1-3/NW	4.00
6	35° 23.150' N	120° 52.496' W	70.7	8:20:51	13.5	100	0.8	2.8	WSW	1-3/NW	4.75
7	35° 23.198' N	120° 52.568' W	77.9	8:46:04	11.9	100	2.1	3.4	WSW	1-3/NW	4.00
8	35° 23.207' N	120° 52.540' W	34.2	8:42:40	12.5	100	2.1	3.4	WSW	1-3/NW	3.75
9	35° 23.189' N	120° 52.517' W	24.6	8:38:33	12.3	100	1.7	2.3	WSW	1-3/NW	4.00
10	35° 23.200' N	120° 52.491' W	16.8	8:35:09	12.3	100	1.8	2.9	WSW	1-3/NW	4.25
11	35° 23.201' N	120° 52.469' W	43.0	8:31:55	12.7	100	1.7	2.7	WSW	1-3/NW	4.00
12	35° 23.201' N	120° 52.434' W	99.3	8:28:50	12.7	100	1.7	2.8	WSW	1-3/NW	4.00
13	35° 23.184' N	120° 52.527' W	50.5	8:58:04	12.8	100	1.3	2.4	WSW	1-3/NW	4.25
14	35° 23.224' N	120° 52.531' W	46.5	8:49:39	12.2	100	1.7	3.0	WSW	1-3/NW	3.90
15	35° 23.224' N	120° 52.472' W	72.1	8:53:10	12.2	100	2.0	3.9	WSW	1-3/NW	4.00
16	35° 23.179' N	120° 52.469' W	38.7	8:25:05	12.8	100	1.4	1.6	WNW	1-3/NW	4.50

There was no visual expression of the effluent plume at the sea surface. Neither odors nor debris of sewage origin were observed at any time during the survey.

Tidal Conditions (Pacific Daylight Time)
High Tide: 02:23 4.13 ft
Low Tide: 09:07 0.52 ft
High Tide: 16:03 4.55 ft
Low Tide: 22:21 1.04 ft